Title: SZ Calibration with the Sunyaev-Zel'dovich Array

Date: Apr 28, 2009 11:45 AM

URL: http://pirsa.org/09040042

Abstract: As observations of clusters through their SZ imprint on the CMB becomes more routine, it is now feasible to add this signal to the set of observables we use to study galaxy clusters. Using the Sunyaev-Zel'dovich Array (SZA), we are pursuing a variety of programs to investigate the correlation between cluster properties and their SZ signatures. I will present early results from these comparisons. The SZA is also a unique tool for resolved SZ imaging as part of the 23-element CARMA interferometer. I will discuss our initial experiment with heterogeneous array interferometry later this year and the future capabilities of the full array.

(Fine-Scale Anisotropy and) SZ Calibration with the Sunyaev-Zel'dovich Array

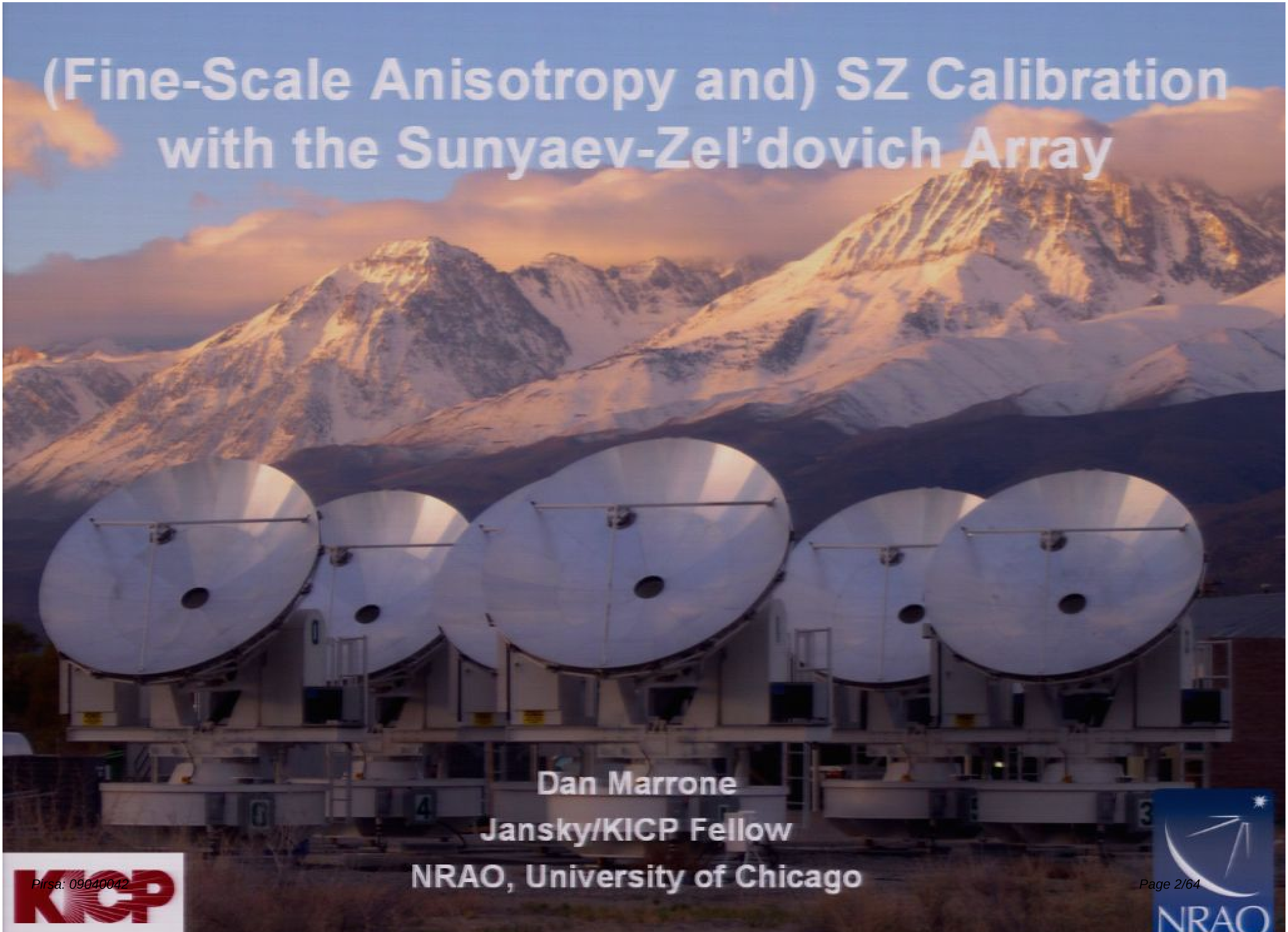

Dan Marrone
Jansky/KICP Fellow
NRAO, University of Chicago

(Fine-Scale Anisotropy and) SZ Calibration with the Sunyaev-Zel'dovich Array

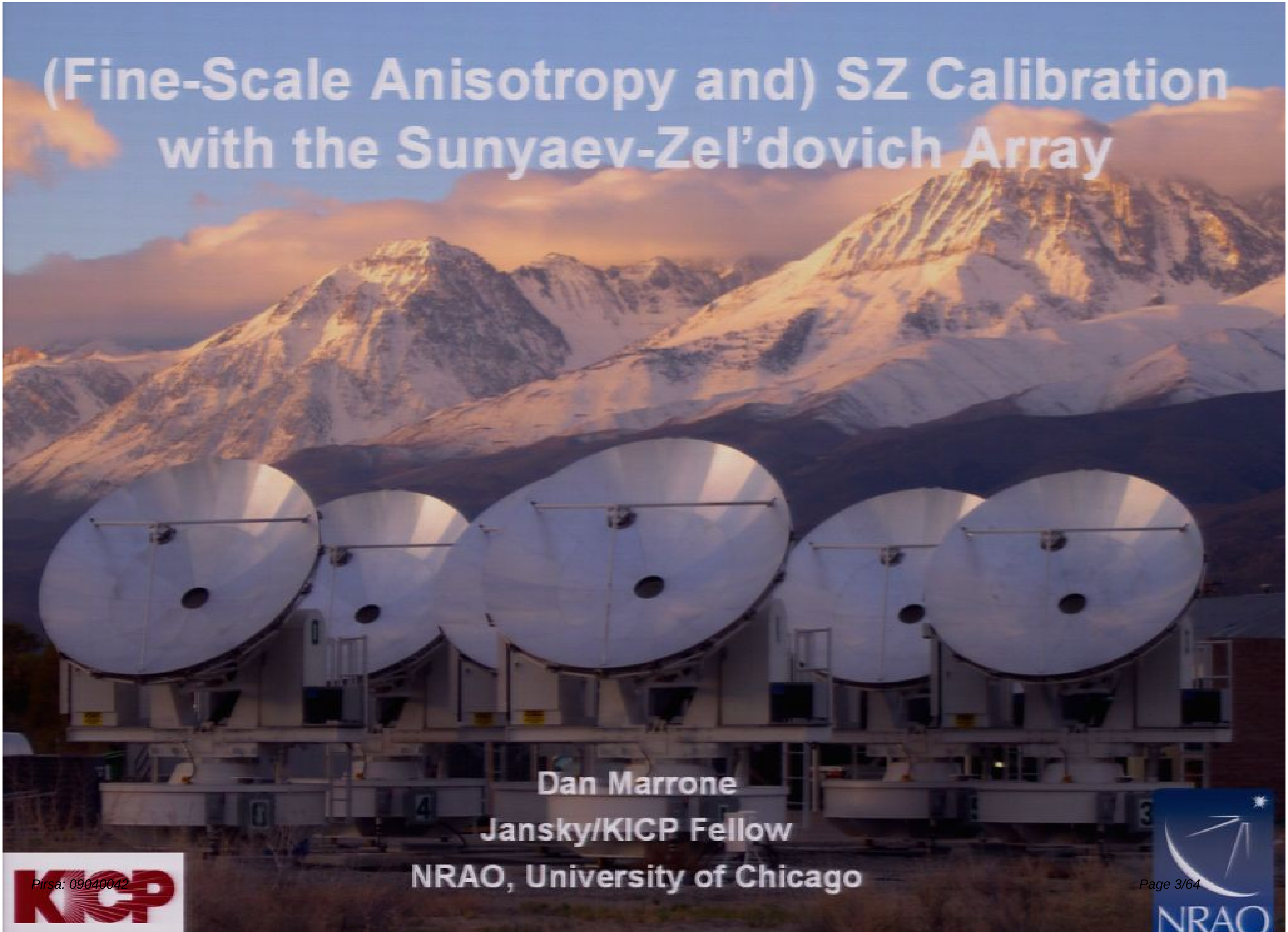

Dan Marrone
Jansky/KICP Fellow
NRAO, University of Chicago

The SZA Collaboration

University of Chicago
John Carlstrom
Tom Culverhouse
Chris Greer
Ryan Hennessy – Nearby Cluster Survey
Erik Leitch
Dan Marrone
Kelsey Morgan
Clem Pryke
Megan Roscioli
Matthew Sharp – CMB Anisotropy
Alan Zablocki

Columbia University
Amber Miller
Tony Mroczkowski – Cluster Modeling
Stephen Muchovej – Blank Field Survey

NASA MSFC
Marshall Joy

University of Alabama, Huntsville
Max Bonamente
Nicole Hasler – Cluster Gas Fraction
Esra Bulbul

Owens Valley Radio Observatory
David Hawkins
James Lamb
David Woody

Former Members
Marcus Runyan
John Cartwright
Michael Loh
Ben Reddall

Funding: NSF, KICP, McDonnell Foundation, UChicago

Student (*2008 Graduate*)
Postdoc

Sunyaev-Zel'dovich Array

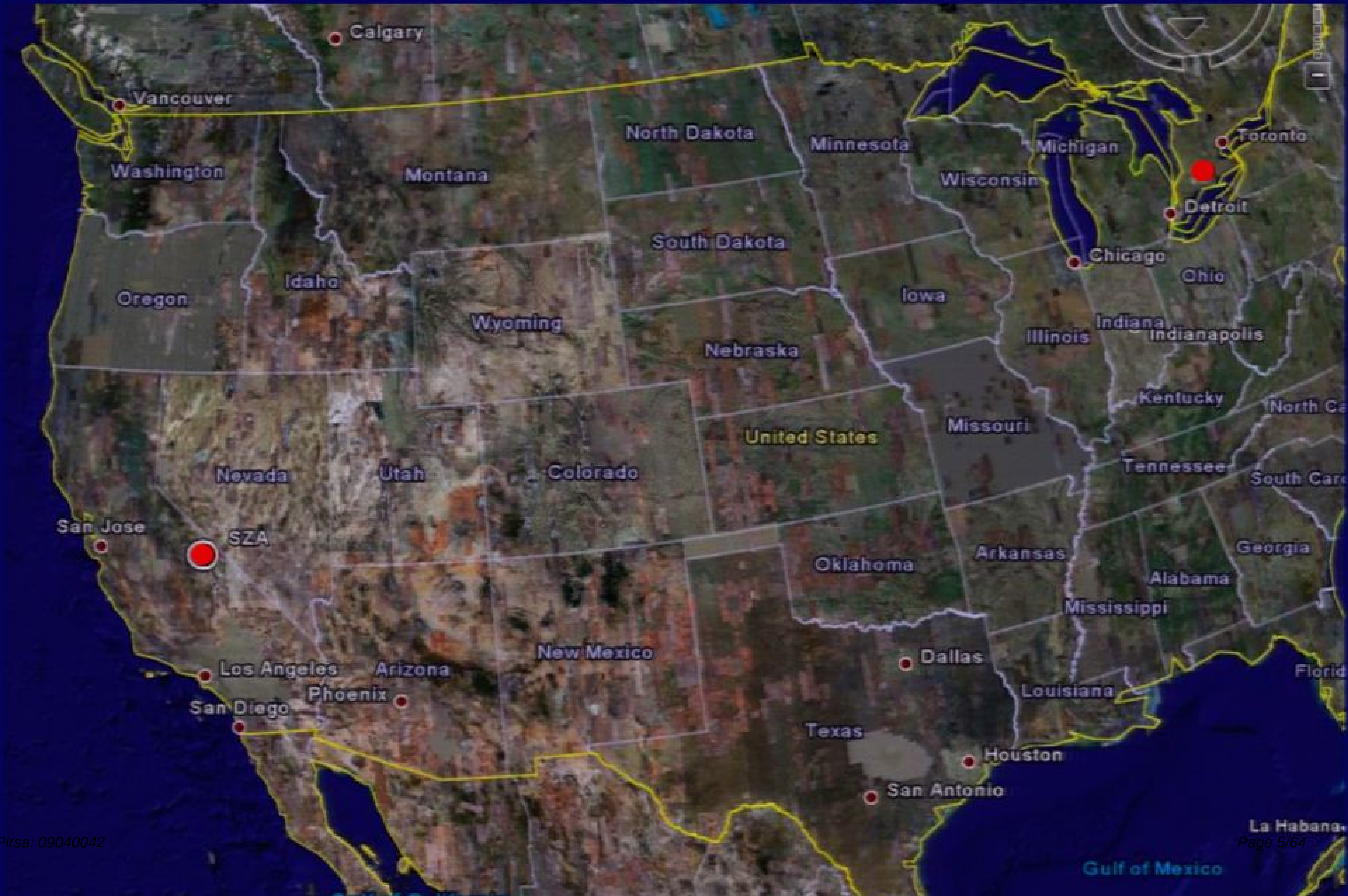

Sunyaev-Zel'dovich Array

8 elements, 3.5m diameter

- Designed for sensitivity to cluster virial radius
- Large bandwidth for high sensitivity: 8 GHz (25% at 30 GHz)
- 6 central antennas for SZ sensitivity, 2 outriggers for contaminant removal

Two frequencies

- 30 GHz: primary observations
- 90 GHz: higher resolution follow up, contamination checks

Science operations began Nov 2005

- 1.5yrs: 6sq deg survey, CMB anisotropy
- Clusters since Sep 2007

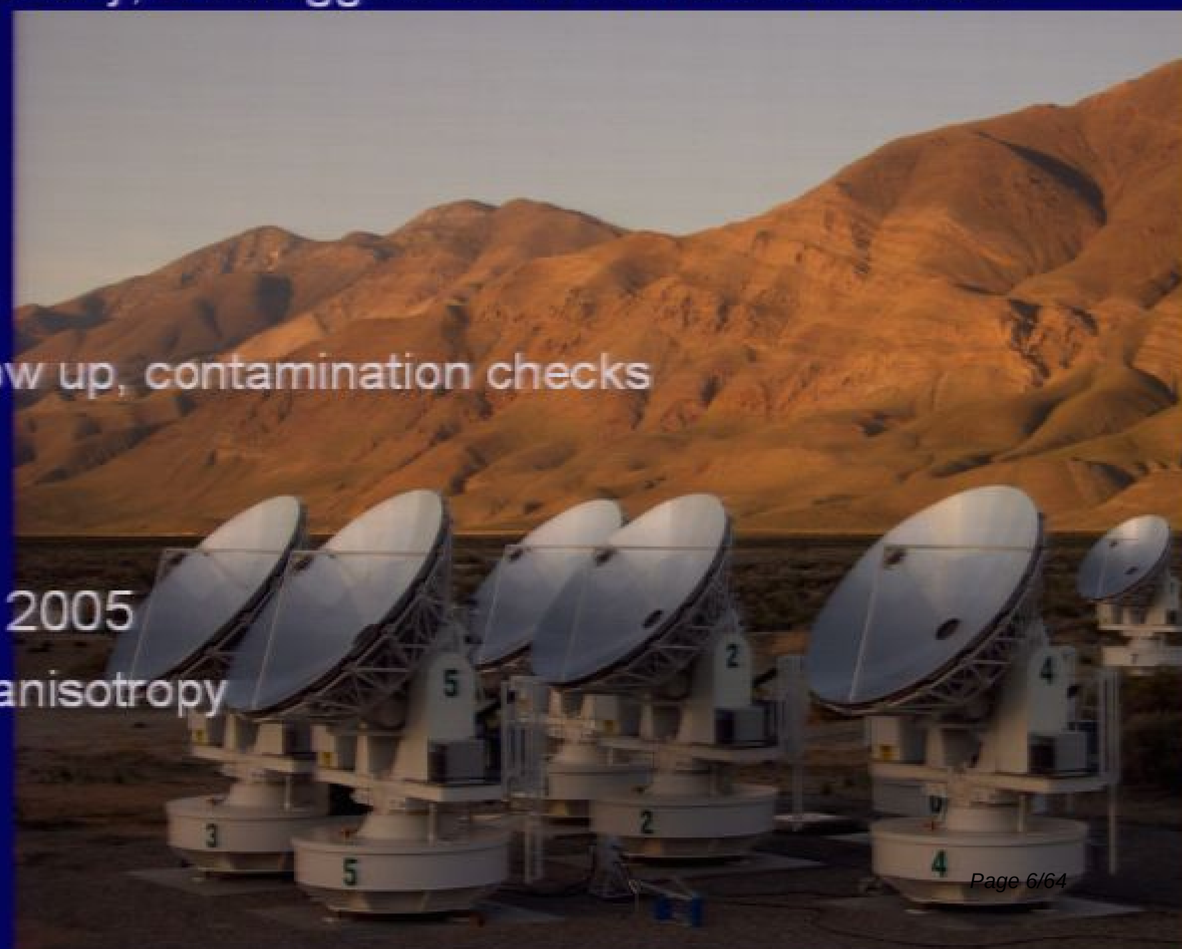

SZA+CARMA

Array moved to CARMA site, July 2008

CARMA: 6x10.4m + 9x6.1m

Merger timeline:

- August 2009: 10+3.5m (14-element) SZ interferometry (10-45" scales)
- *Proposals to SZA through CARMA TAC* – Mar/Sep 2009
- Full array combination – 2010-2011

SZA+CARMA

What can we do with this array?

Sensitivity, angular resolution, dynamic range all significantly improved

Detailed cluster imaging becomes possible

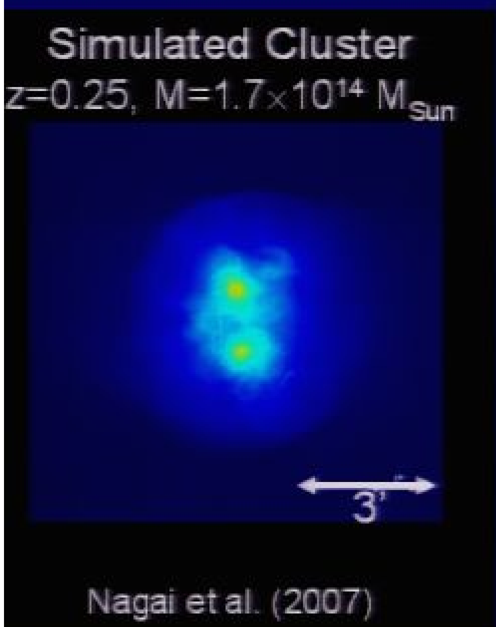

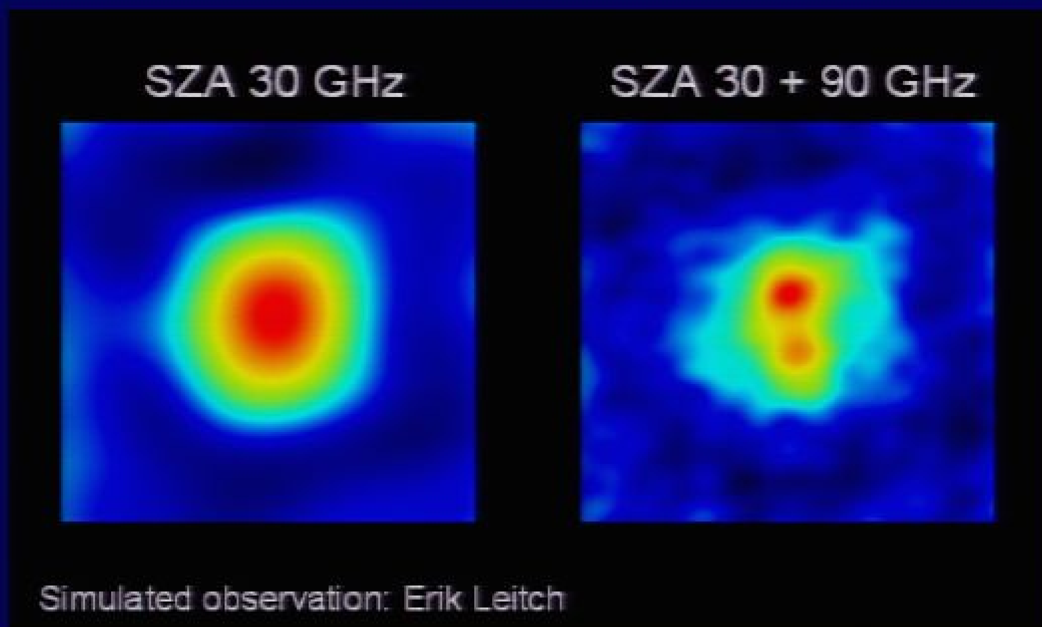

SZA+CARMA

What can we do with this array?

Sensitivity, angular resolution, dynamic range all significantly improved

Detailed cluster imaging becomes possible

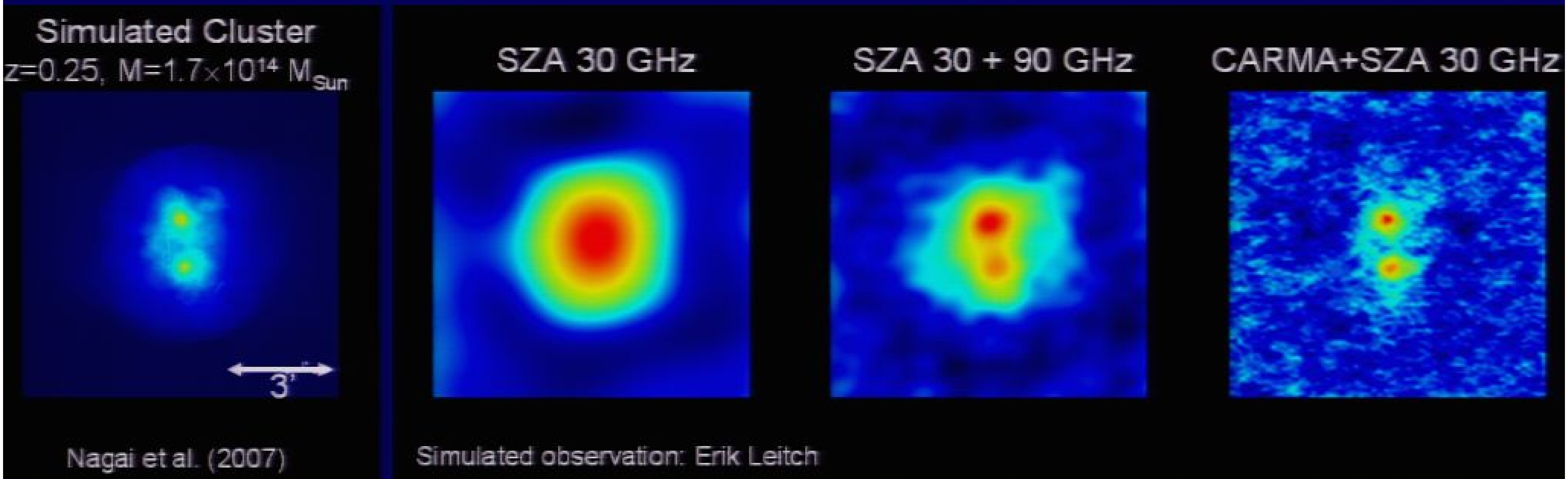

Understanding the SZ Signal

SZ survey telescopes will primarily survey, not study

- This may be okay, large cluster samples provide many ways to "self-calibrate" the mass-observable relation

Specialized instruments can make important contributions here

- Control over systematics
- Higher-resolution imaging capabilities
- Extensive multi-wavelength data for smaller cluster sample

Local Cluster Substructure Survey (LoCuSS)

PI: Graham Smith (Birmingham)

LoCuSS

Morphologically unbiased, X-ray selected, z=0.15-0.3

- Strong lensing – HST/ACS+WFPC2, Keck
- Weak lensing – Subaru
- X-ray – XMM/Chandra
- SZ – SZA/CARMA
- UV – star formation – GALEX
- Near-infrared – stellar mass maps – Palomar+NOAO
- Spitzer/MIPS – AGN/SF 24um
- Far-infrared – Star formation – Herschel Key Project

Local Cluster Substructure Survey (LoCuSS)

68 Clusters observed with SZA (so far)

- ~50 with X-ray, ~40 with weak lensing, ~50 with strong lensing

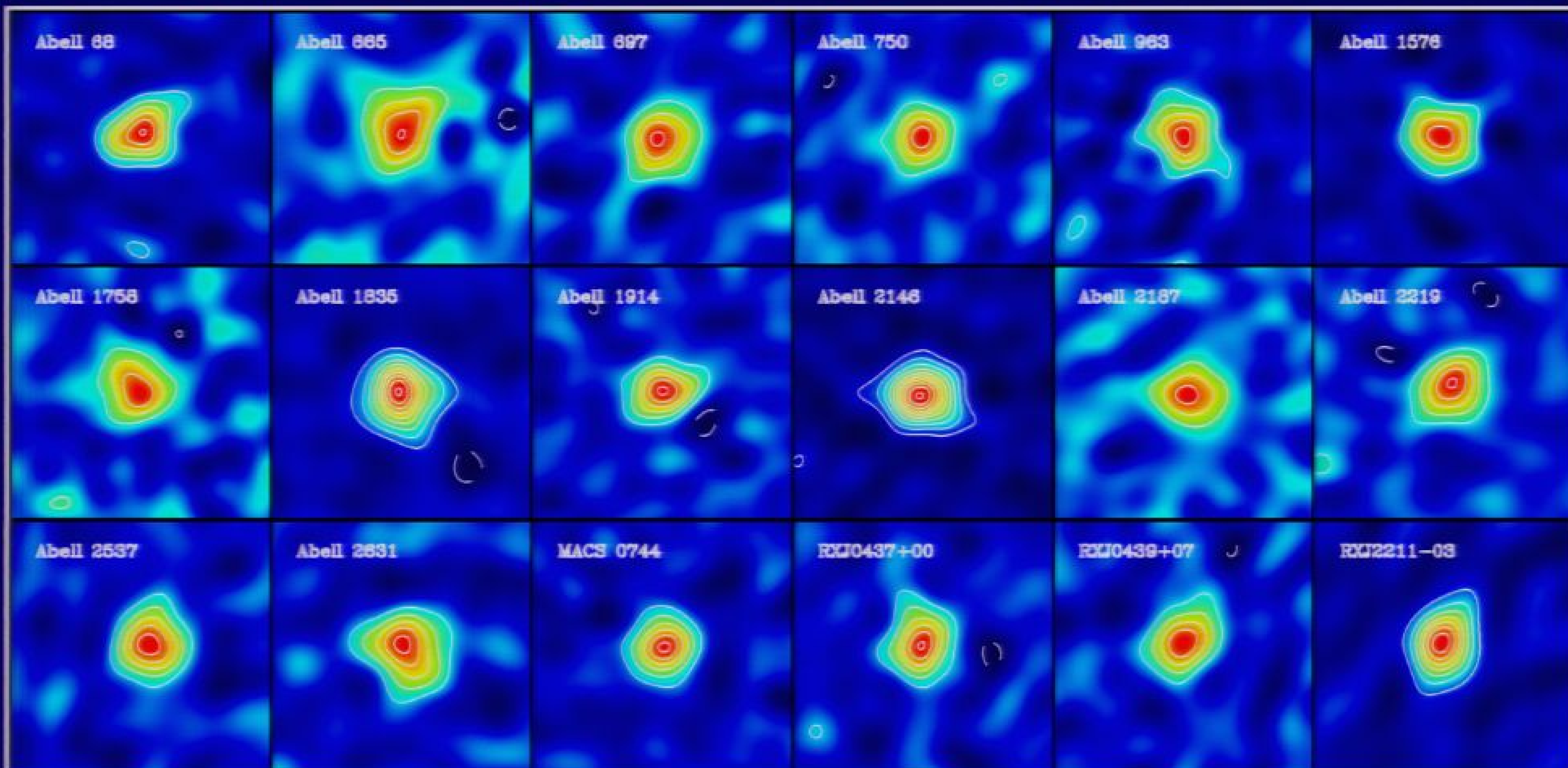

Local Cluster Substructure Survey (LoCuSS)

Major SZ projects:

- Scaling relations, calibration of SZ systematics:
  - Examine scatter in Mass – Y relationship from core to virial radius
  - Determine hydrostatic mass bias
  - Effects of morphology/merging on SZ signal
- Feedback to cluster simulations
- Covariance of observables (SZ/X-ray/Mass)

First SZA+LoCuSS Results

- ICM Gas: $Y_X - Y_{SZ}$
- $M_{WL} - Y_{SZ}$

First SZA+LoCuSS Results: Y_X–Y_{SZ}

Kravtsov et al. (2006) introduced an X-ray analogue for SZ signal

$$Y_X = M_{g,\Delta_c} T_X.$$

Constructed from X-ray observables (M, T)

Pressure-like, should behave like SZ

Simulations show tight M-Y_X correlation

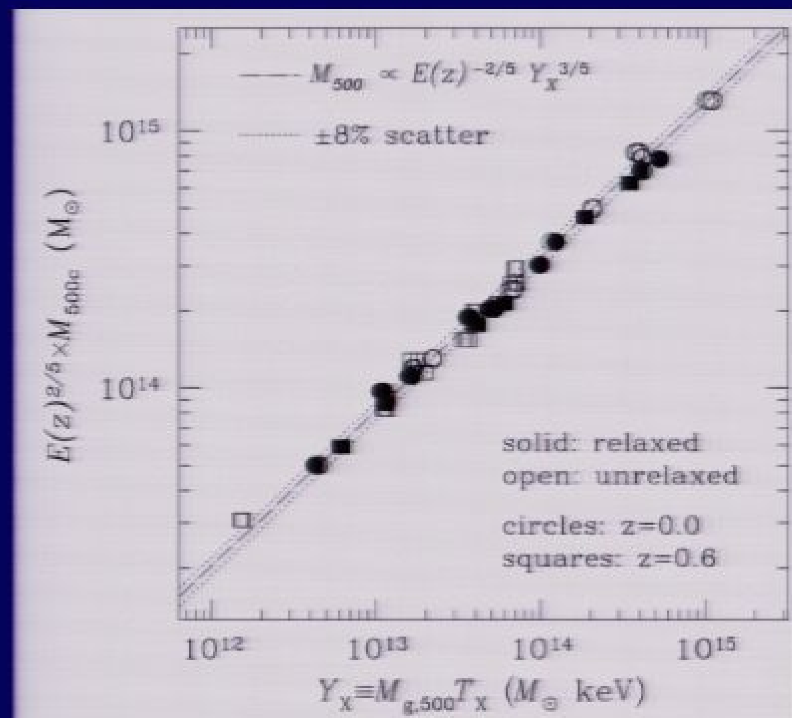

Simulated M vs. Y_X – Kravtsov et al. (2006)

First SZA+LoCuSS Results: Y_X–Y_{SZ}

X-ray analysis of 35 LoCuSS XMM clusters published (Zhang et al. 2008)

All of these (north of δ=-14°) observed with SZA

Compare Y_{SZ} and Y_X

(DPM, Zhang, Joy, Bonamente, Hasler et al)

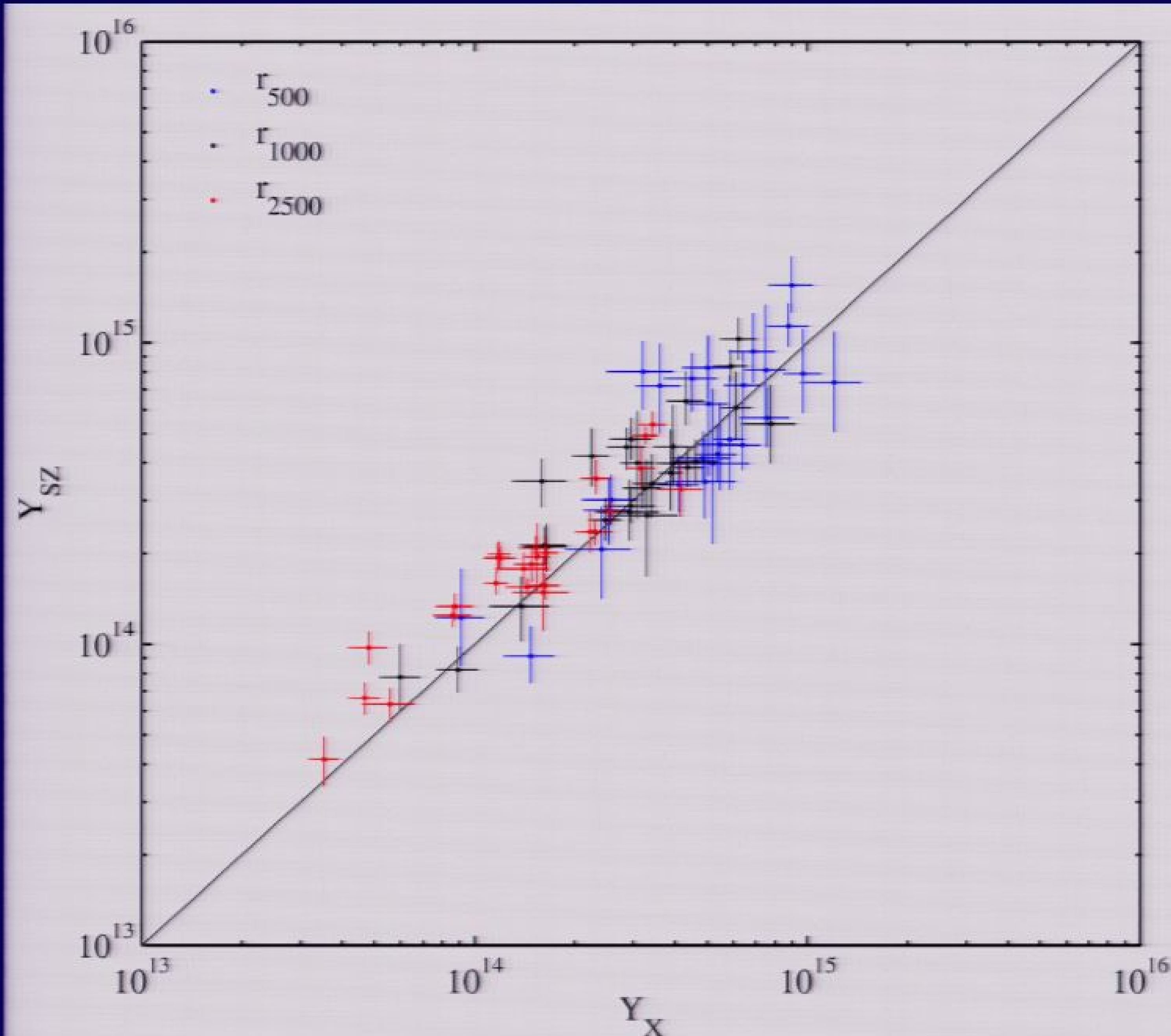
10^{16}
10^{15}
10^{14}
10^{13}
r_{500}
r_{1000}
r_{2500}
Y_{SZ}
Y_X

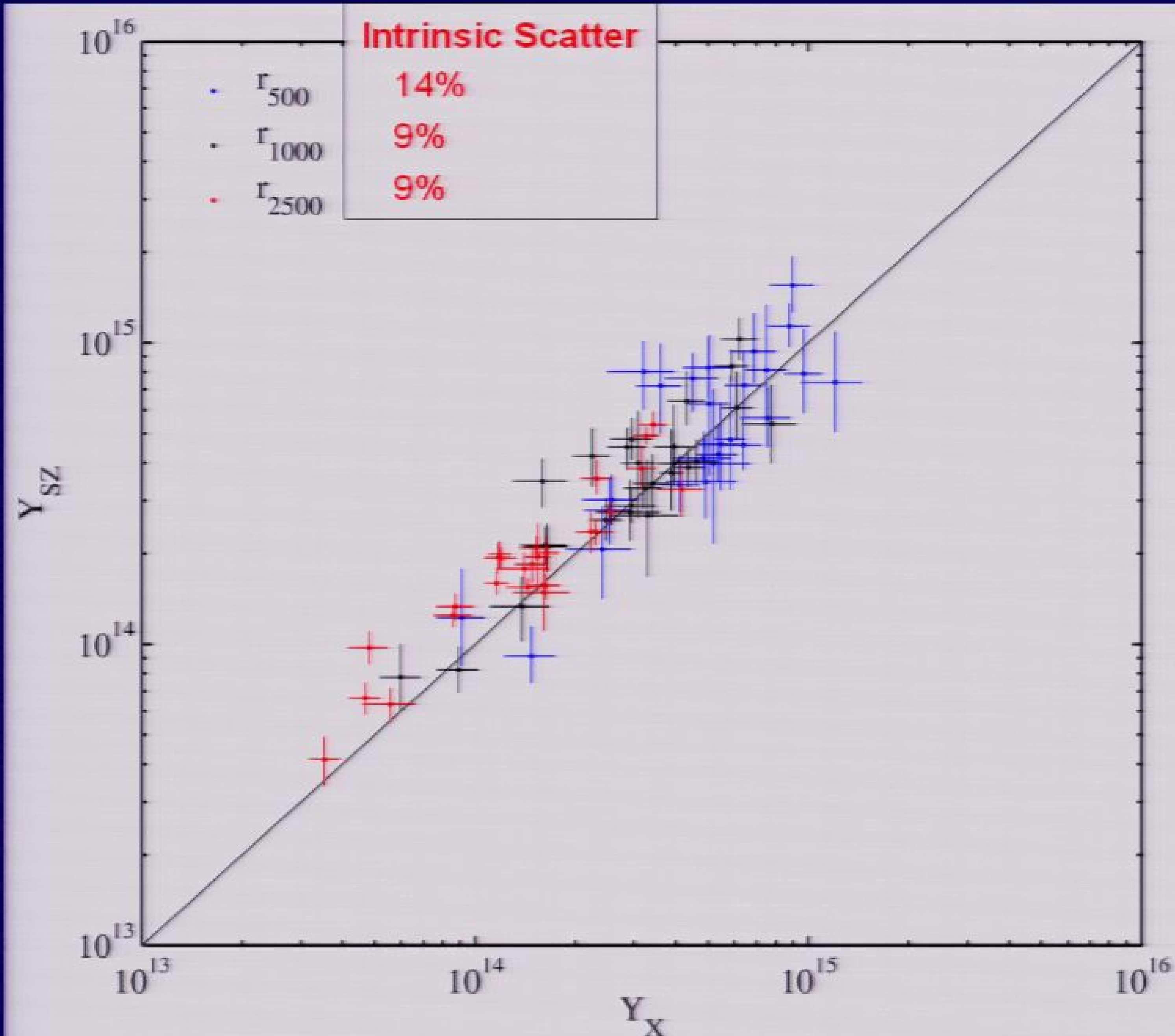
Intrinsic Scatter
r_{500} 14%
r_{1000} 9%
r_{2500} 9%
Y_{SZ}
Y_X
10^{13}
10^{14}
10^{15}
10^{16}

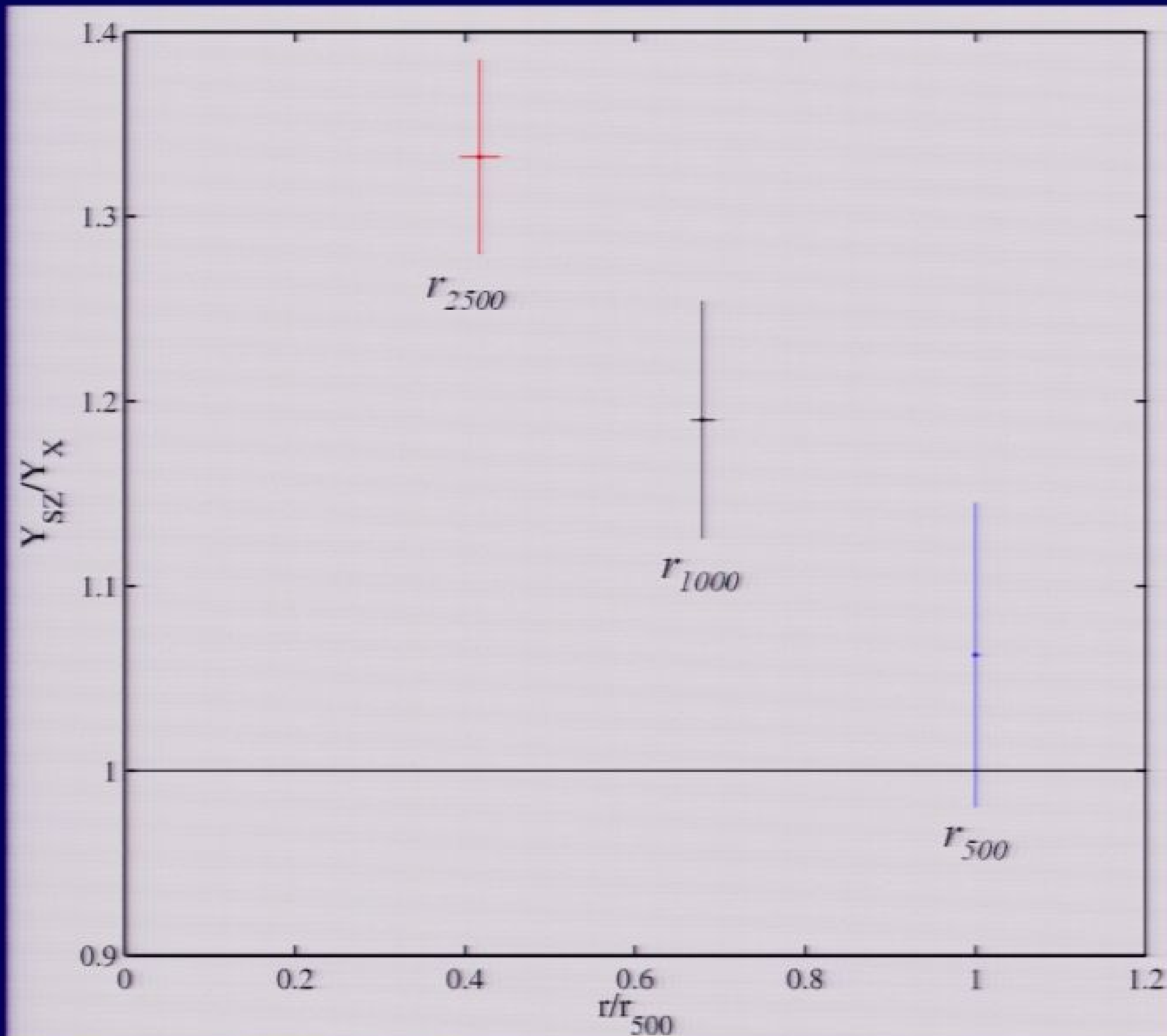

1.4
1.3
1.2
1.1
1
0.9
Y_{SZ}/Y_X
r_{2500}
r_{1000}
r_{500}
0
0.2
0.4
0.6
0.8
1
1.2
r/r_{500}

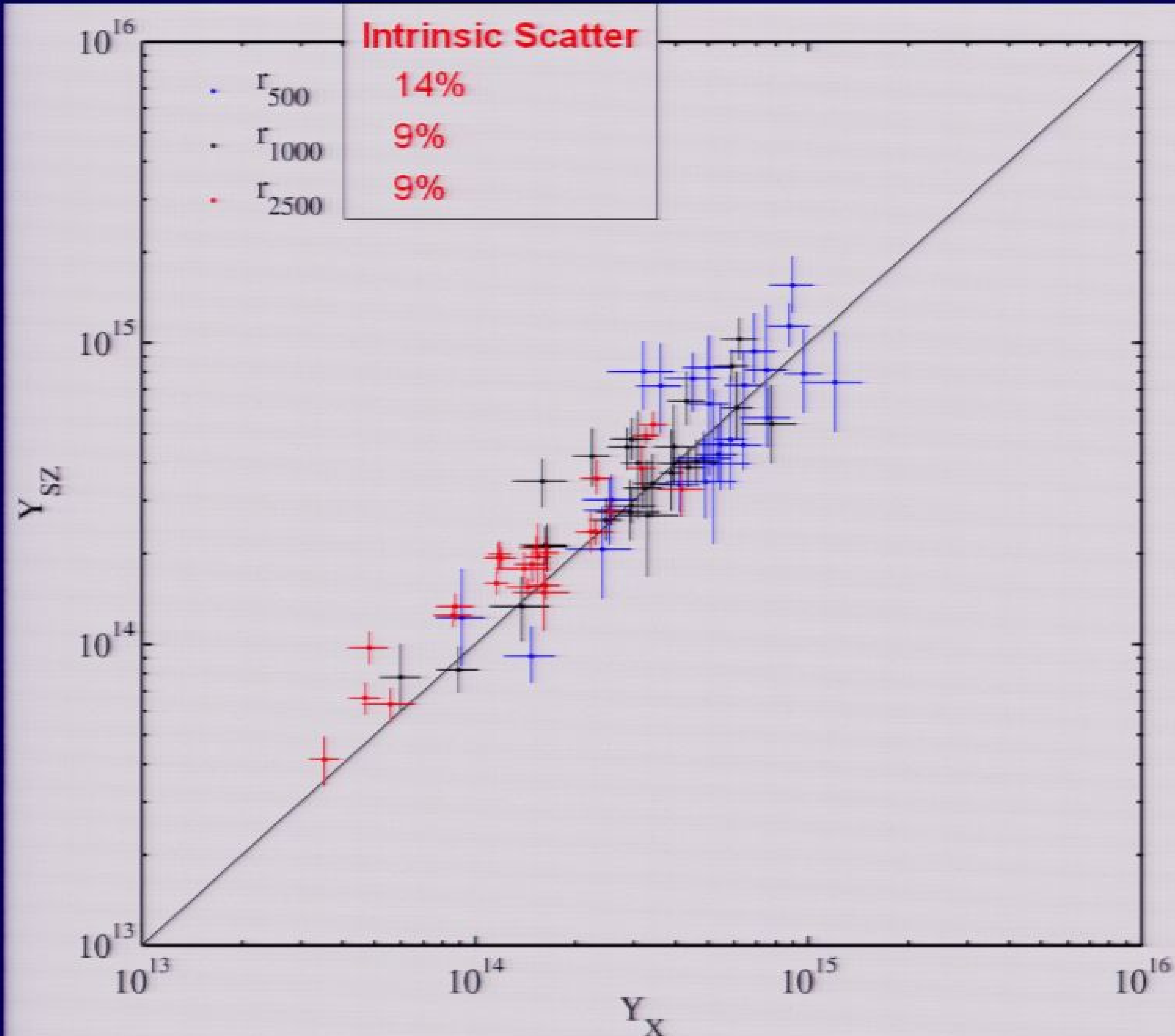

Intrinsic Scatter
r_{500} 14%
r_{1000} 9%
r_{2500} 9%
Y_{SZ}
Y_X
10^{13}
10^{14}
10^{15}
10^{16}

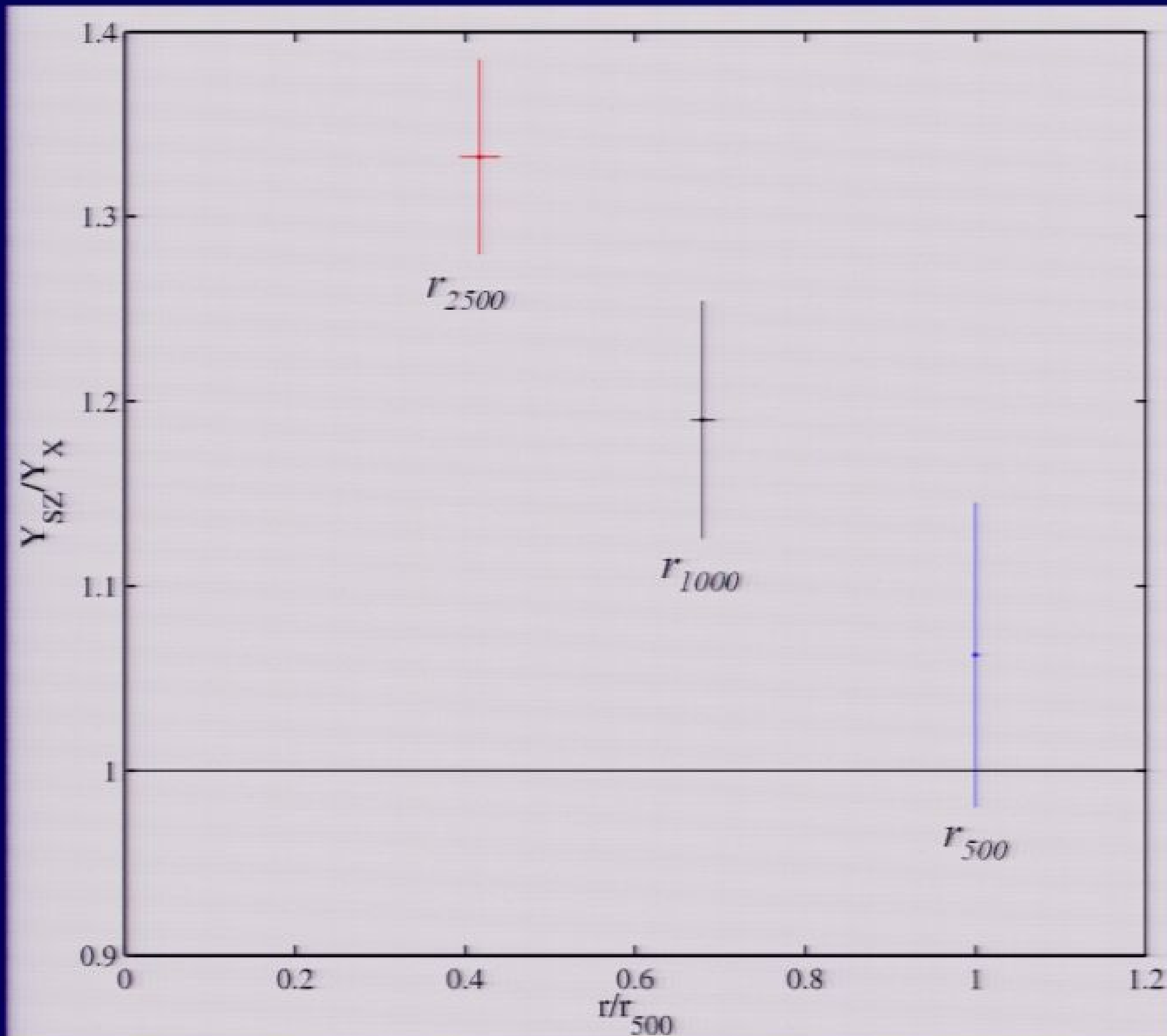
r_{2500}
r_{1000}
r_{500}
Y_{SZ}/Y_X
r/r_{500}
1.4
1.3
1.2
1.1
1
0.9
0
0.2
0.4
0.6
0.8
1
1.2

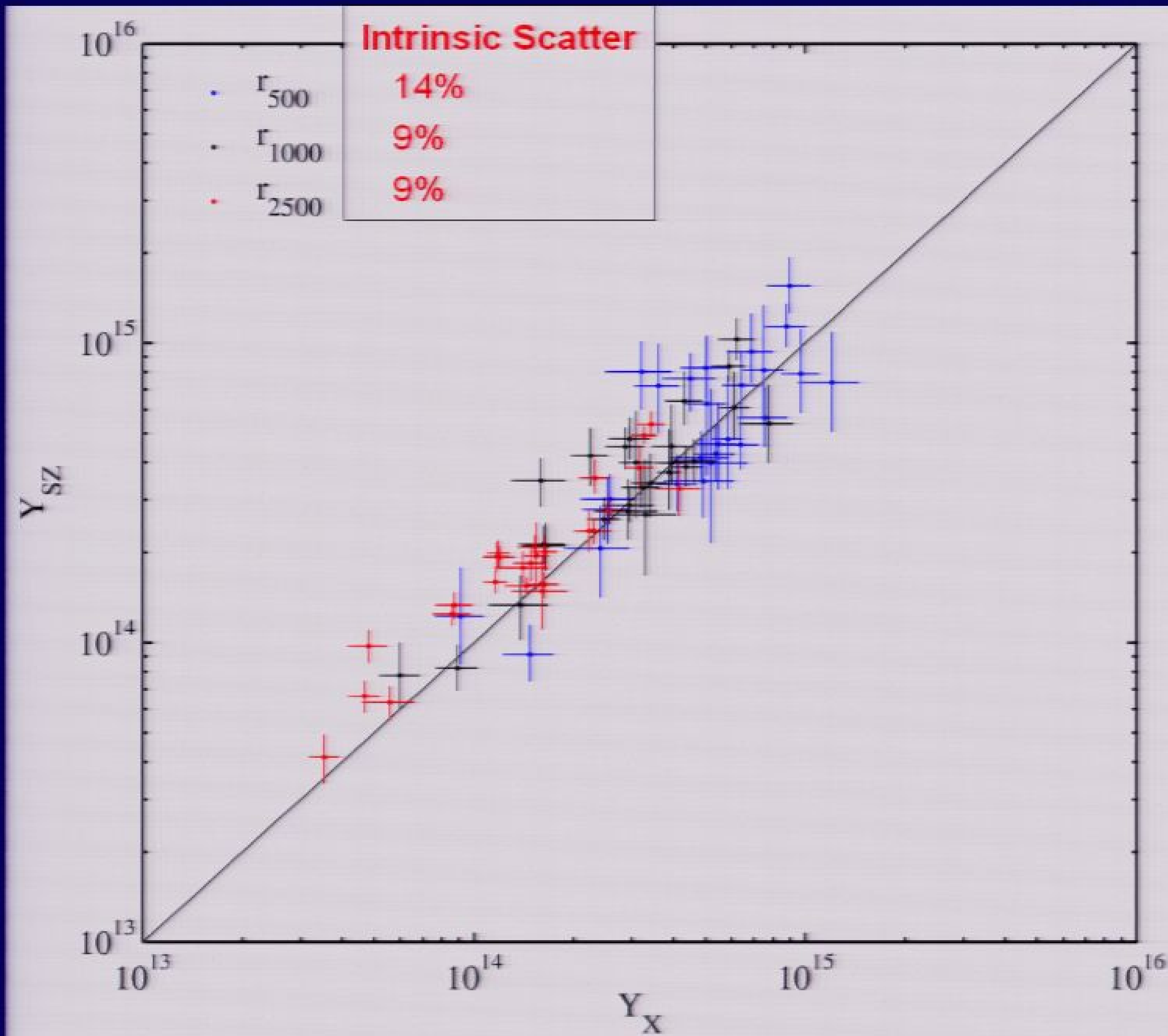
Intrinsic Scatter
r500 14%
r1000 9%
r2500 9%
Y_SZ
Y_X
10^13
10^14
10^15
10^16

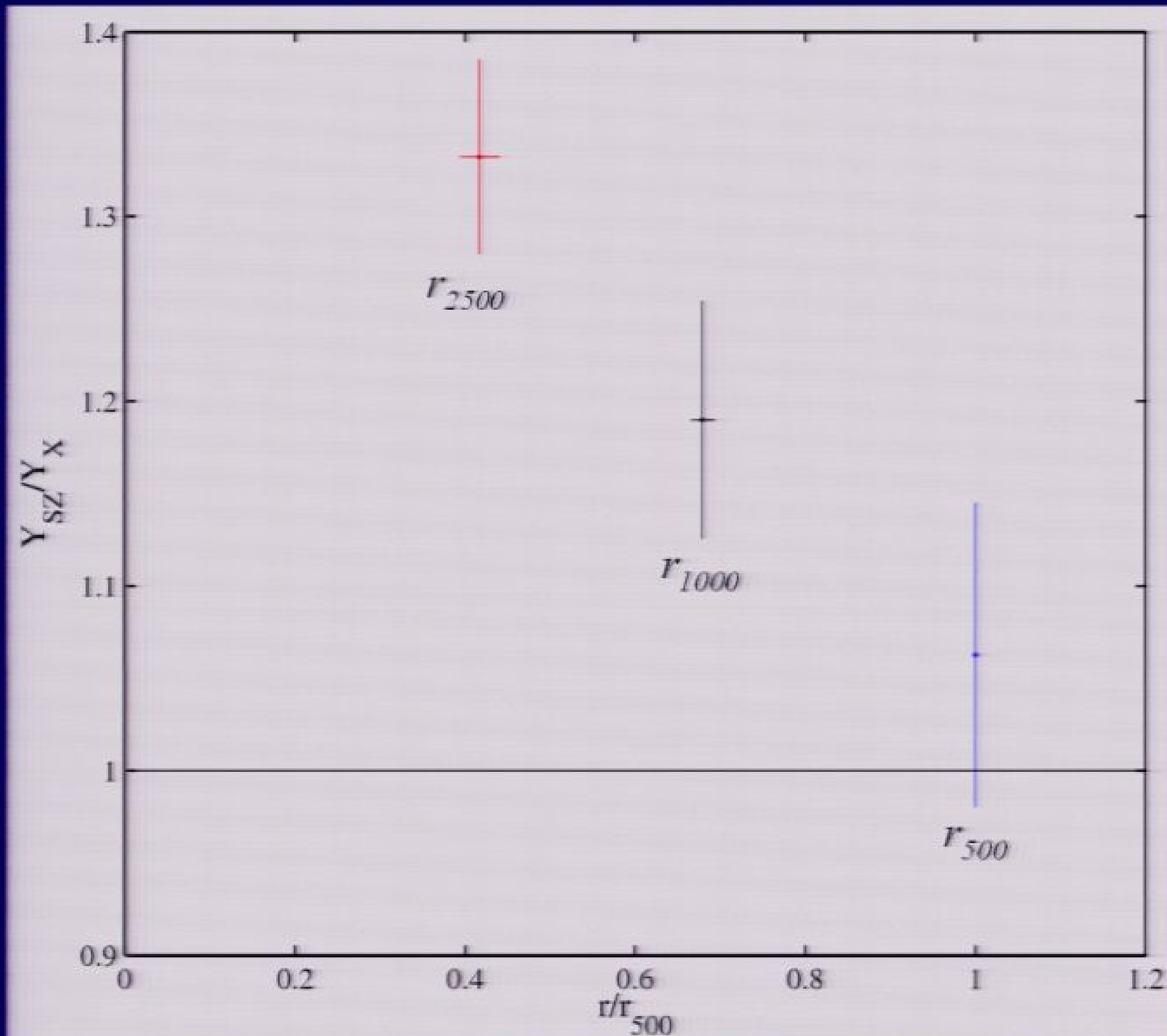

1.4
1.3
1.2
1.1
1
0.9
Y_{SZ}/Y_X
r_{2500}
r_{1000}
r_{500}
0
0.2
0.4
0.6
0.8
1
1.2
r/r_{500}

Cool-Core vs. Non-Cool Core

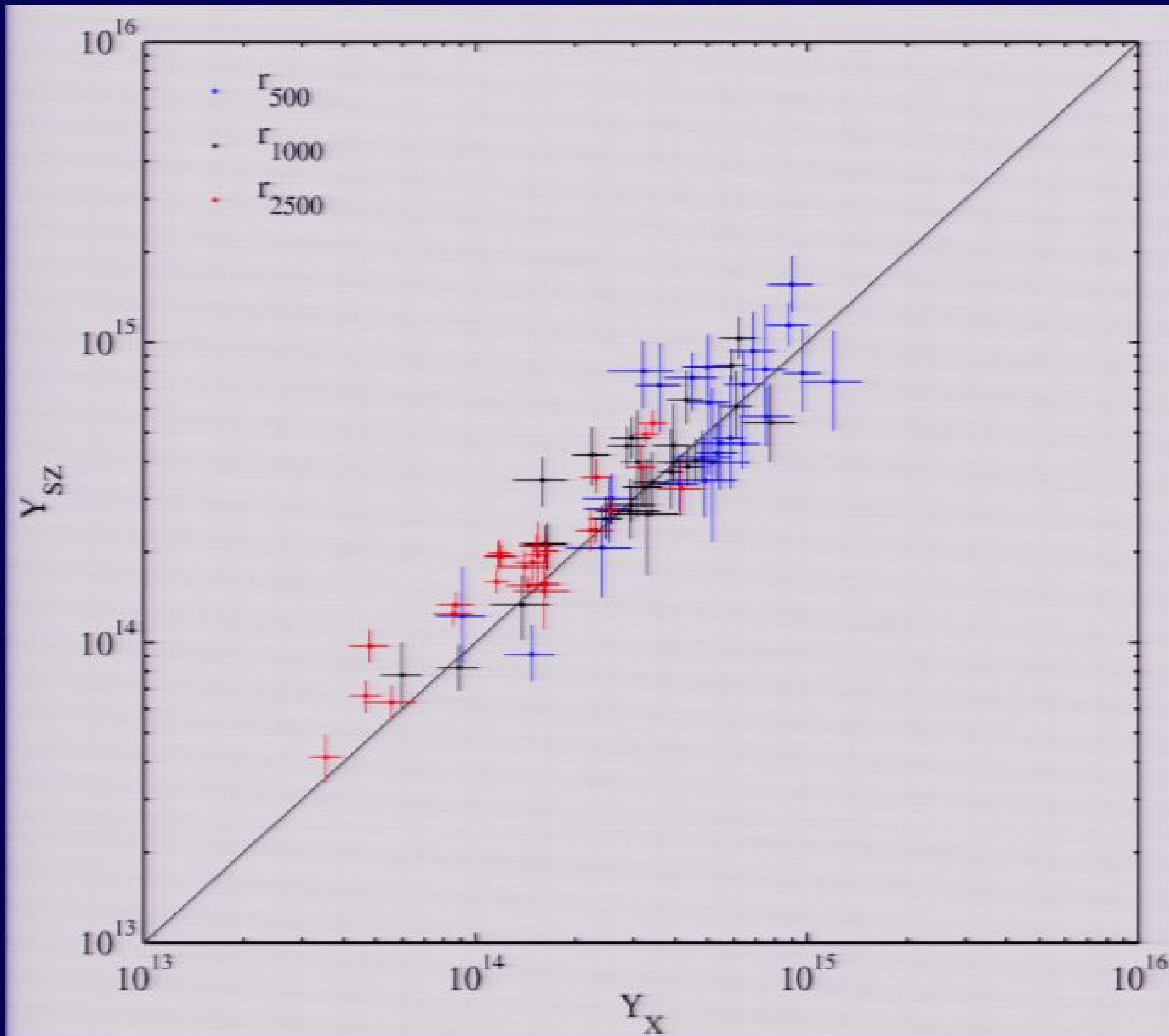

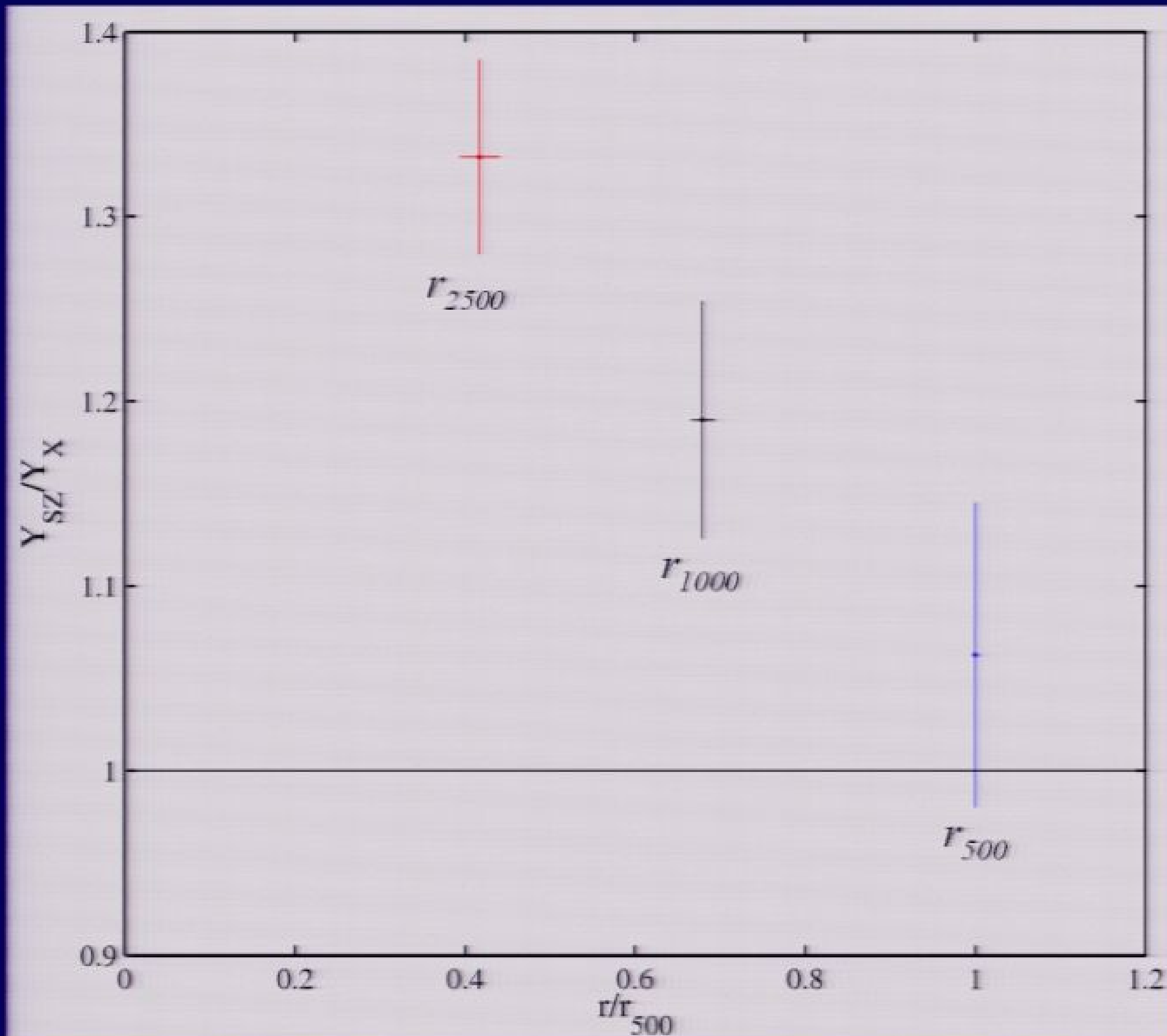

1.4
1.3
1.2
1.1
1
0.9
Y_{SZ}/Y_X
r_{2500}
r_{1000}
r_{500}
0
0.2
0.4
0.6
0.8
1
1.2
r/r_{500}

Cool-Core vs. Non-Cool Core

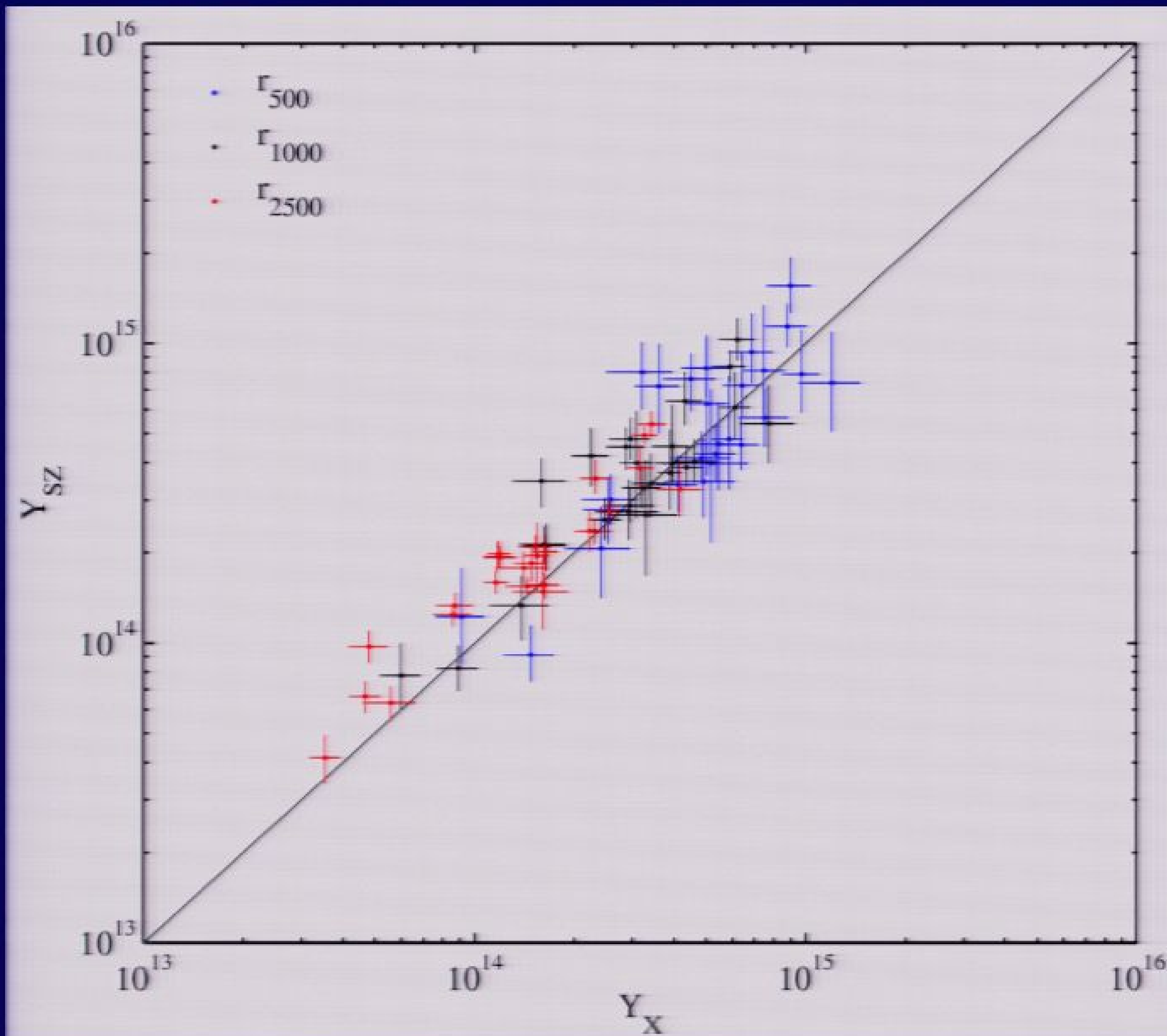

Cool-Core vs. Non-Cool Core

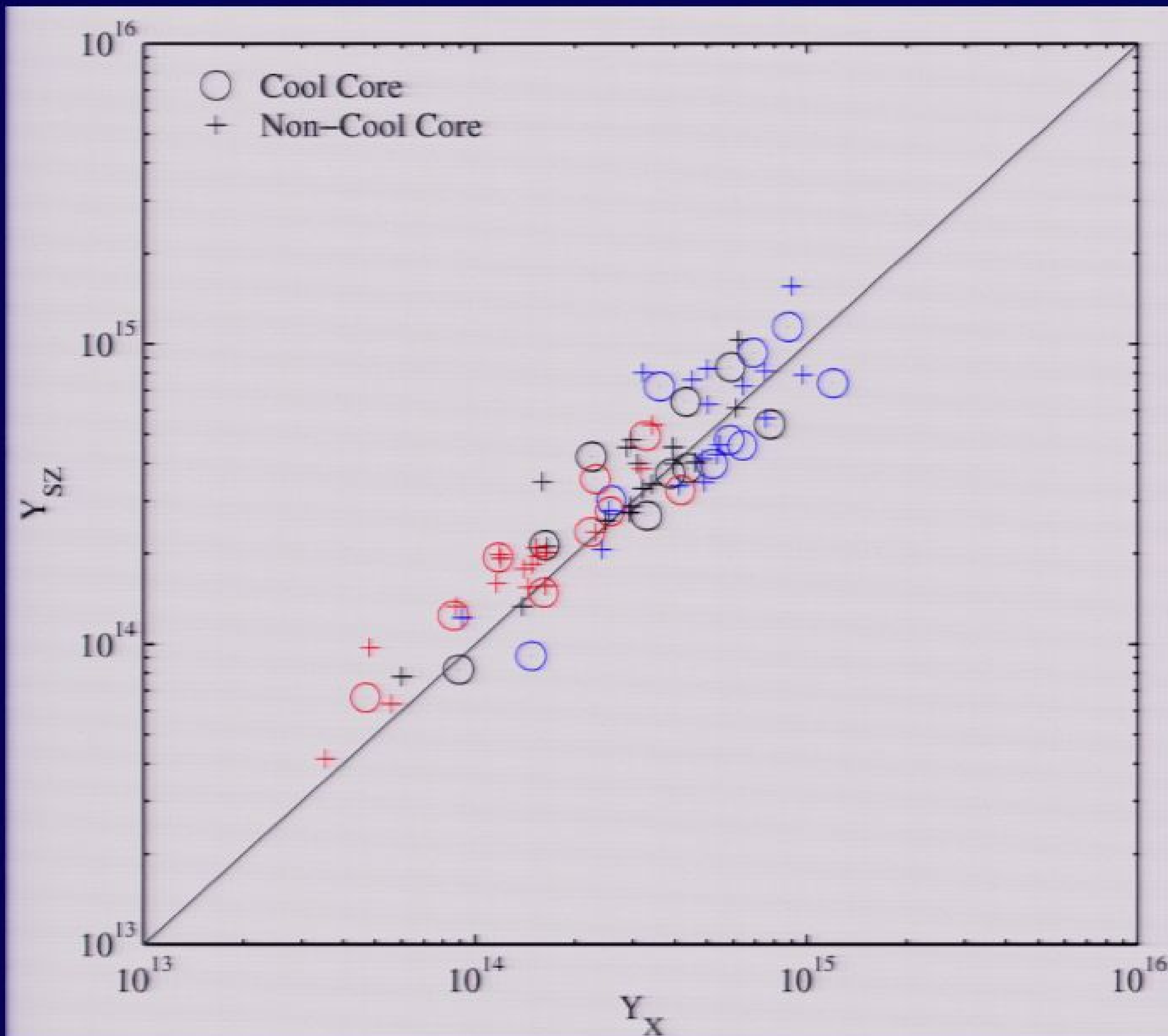

Relaxed vs. Unrelaxed

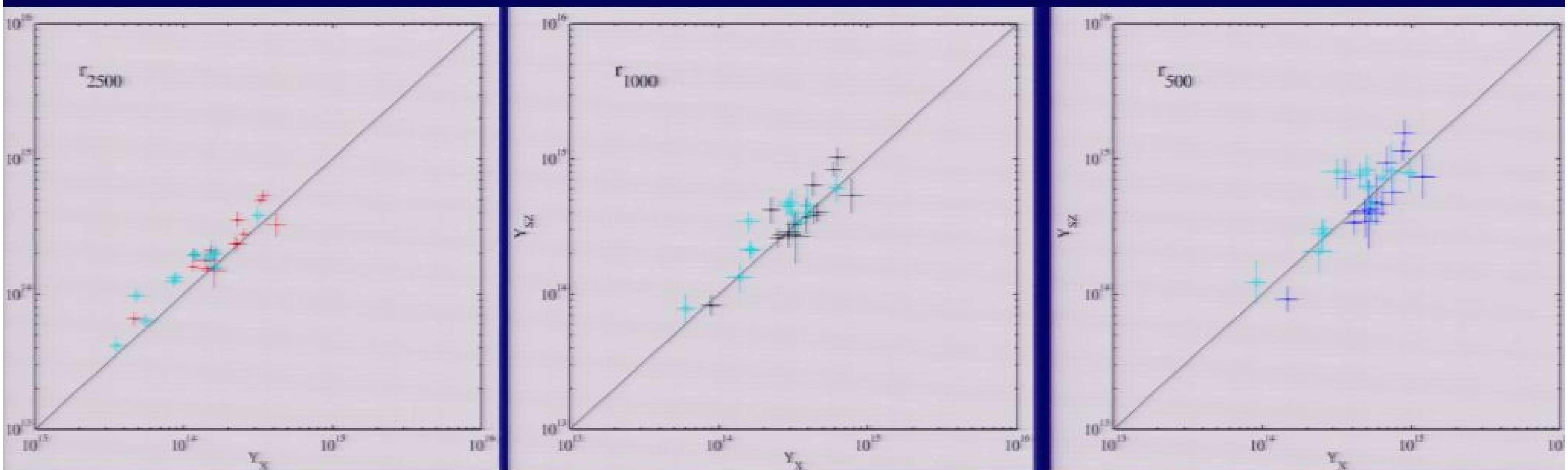

Relaxed vs. Unrelaxed

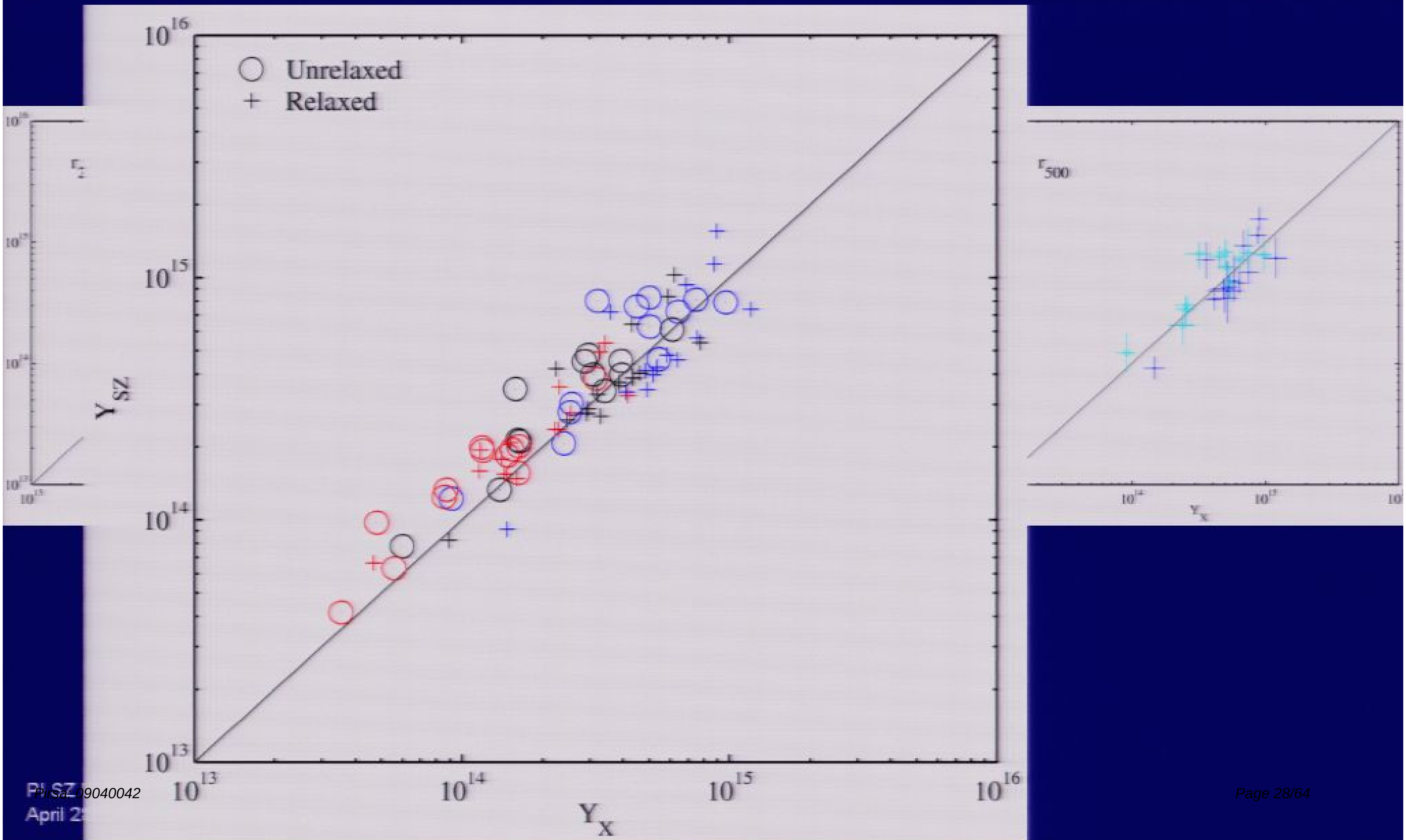

Relaxed vs. Unrelaxed

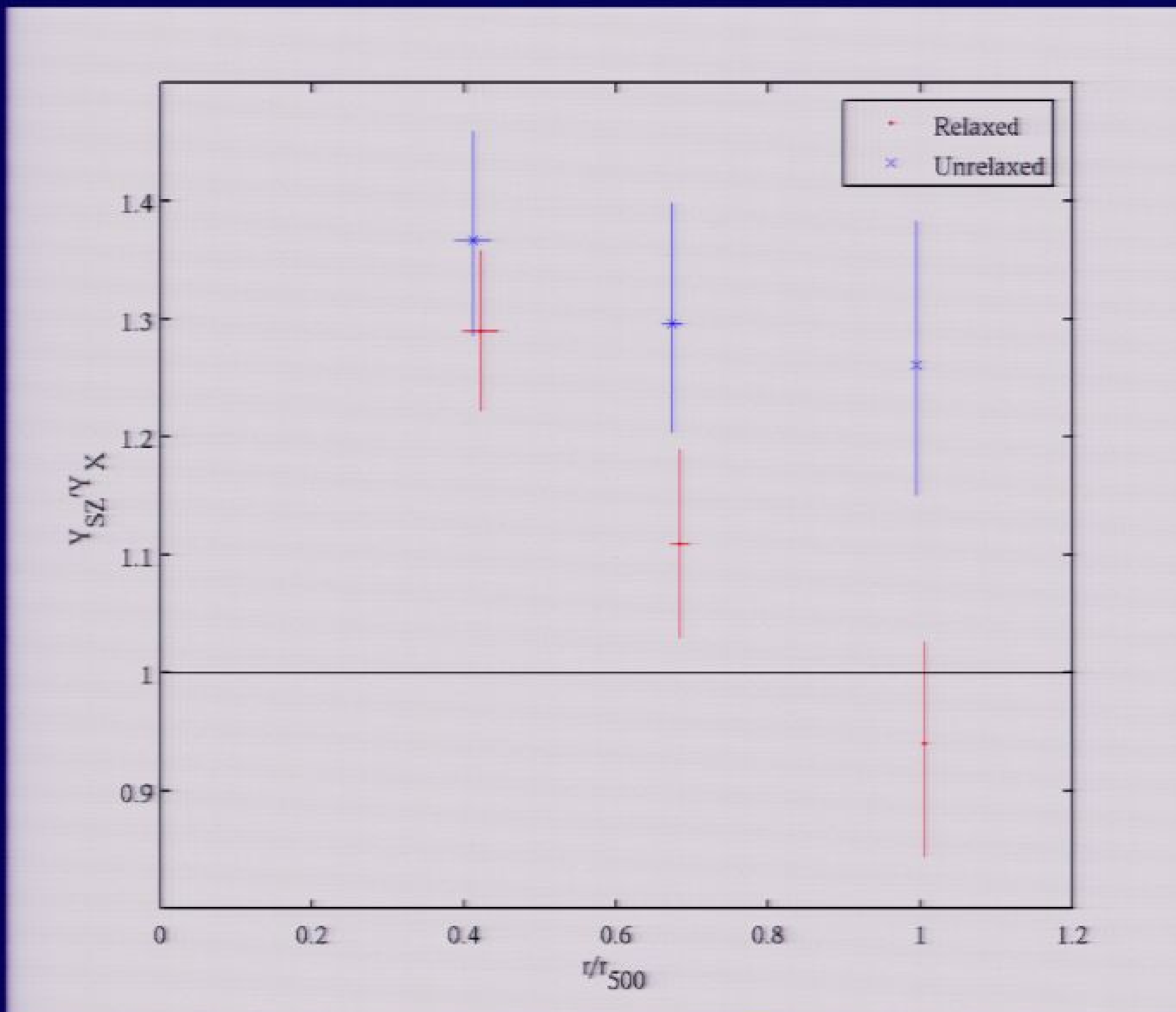

Mass – Y Scaling Relation

Key ingredient for SZ cluster survey cosmology

- Little observational constraint to date
- M-Y scatter unconstrained

Bonamente et al. (2008):

- 38 clusters
- Y from SZ(+X-ray) versus X-ray hydrostatic Mass at r_{2500}
- Measurement errors too large to constrain scatter

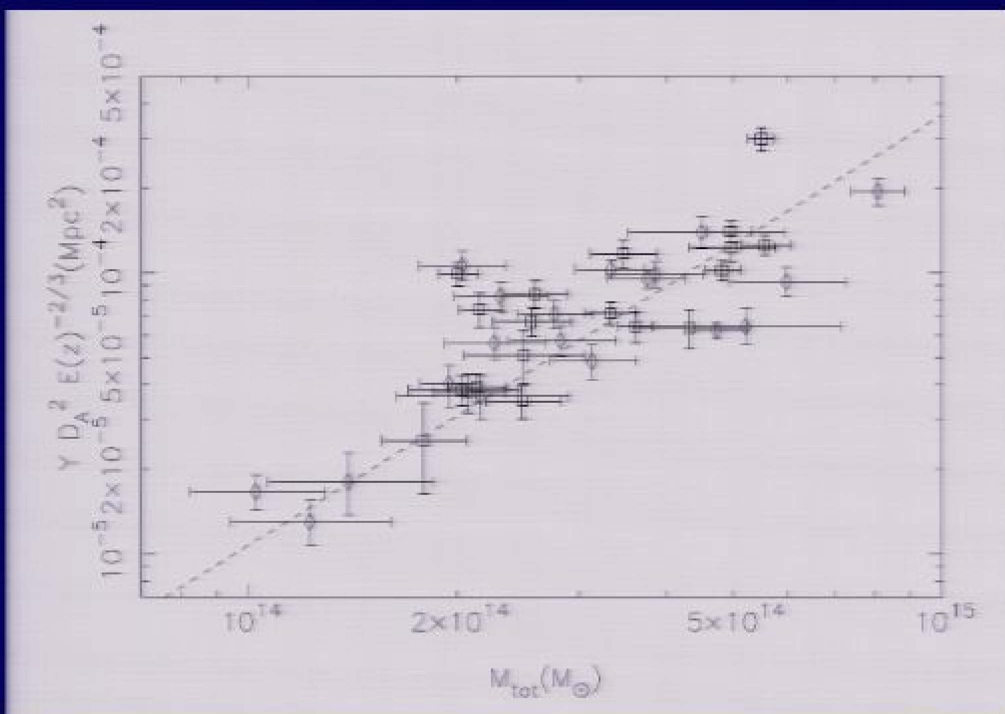

First SZA+LoCuSS Results: M_{WL} – Y

LoCuSS Subaru weak lensing observations provide mass out to r_{vir}

With these data, plus existing X-ray:

- Examine M-Y scaling versus radius
- Check self-similarity
- Measure hydrostatic bias
- Measure scatter
- Examine morphological (merger state) effects

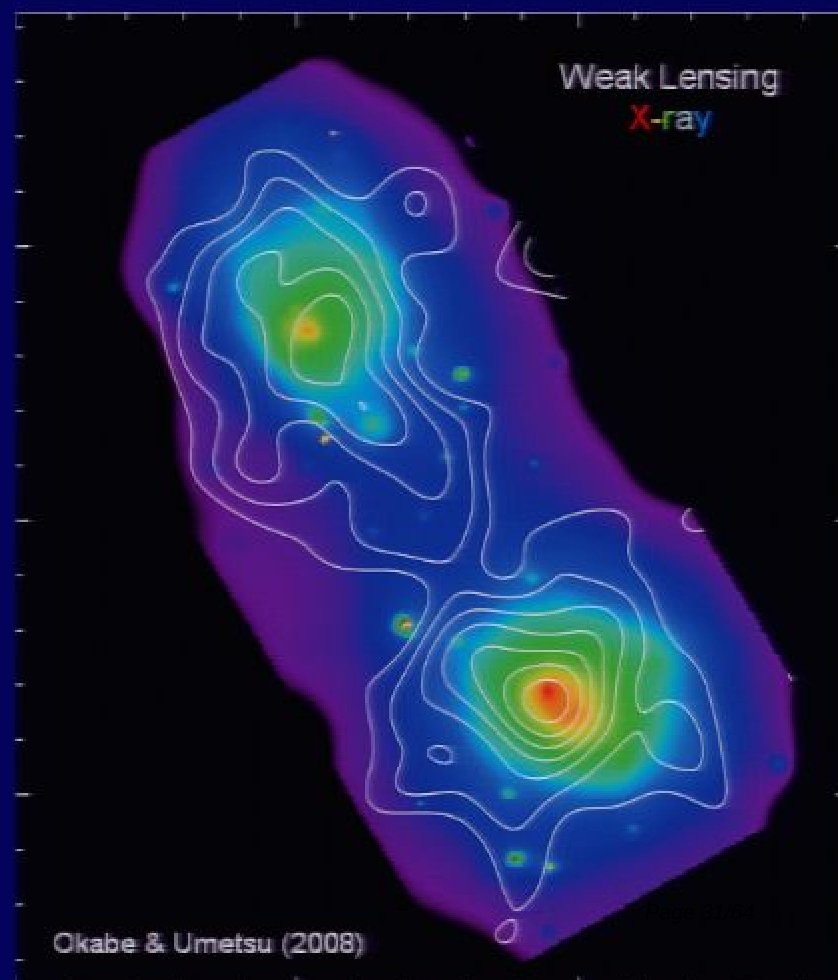

First SZA+LoCuSS R

LoCuSS Subaru weak lensing ob

With these data, plus existing X-r

- Examine M-Y scaling versus
- Check self-similarity
- Measure hydrostatic bias
- Measure scatter
- Examine morphological (merger state) effects

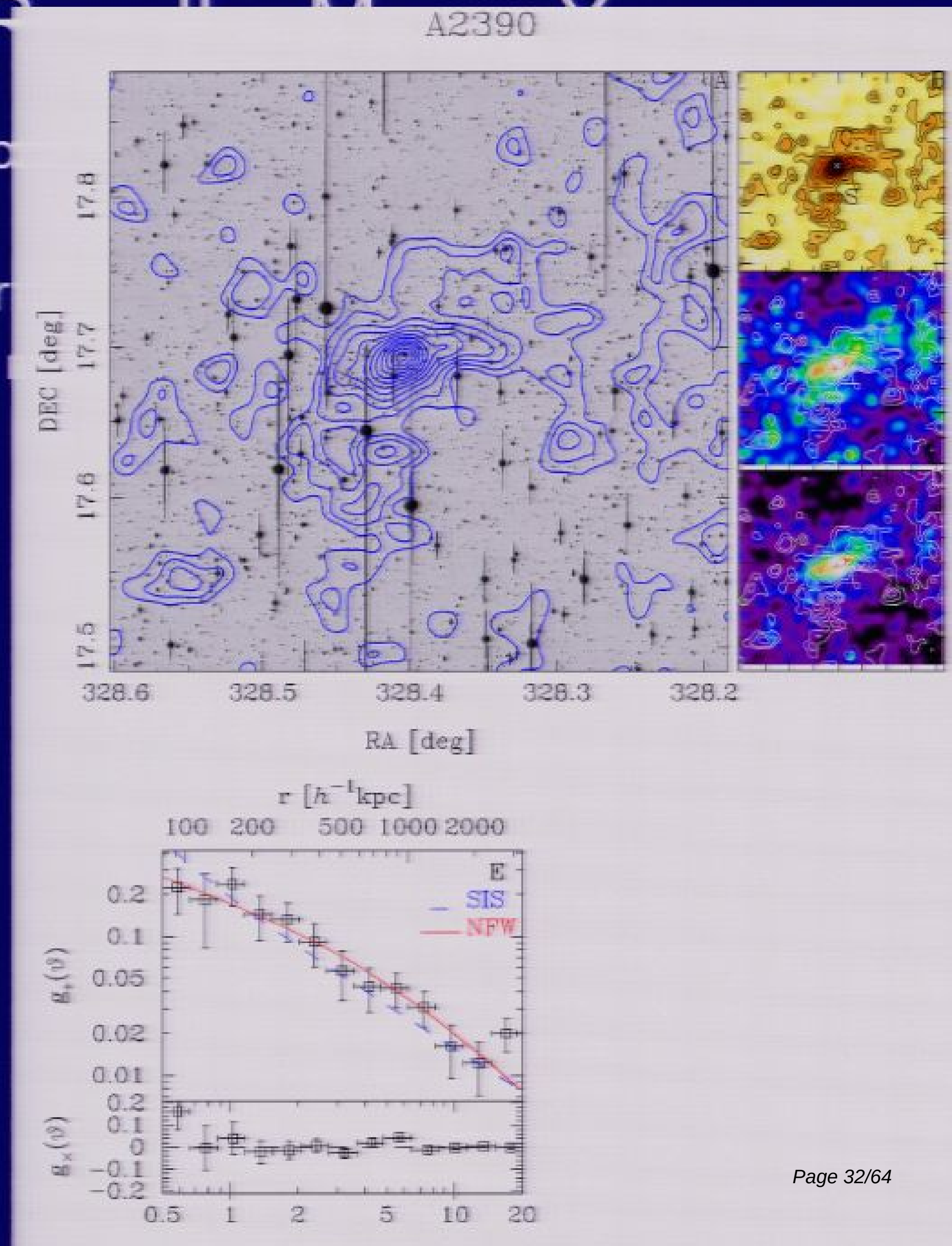

LoCuSS: Subaru Weak Lensing

Okabe et al. 2009, PASJ, submitted

30 cluster sample, two-band imaging

22 clusters with weak shear profiles well-fit by NFW

- 8 with no clear mass concentration, poor NFW/SIS fit

$\Delta M/M \sim 0.15\text{-}0.5$ →

- Best at $r_{2500} - r_{500}$

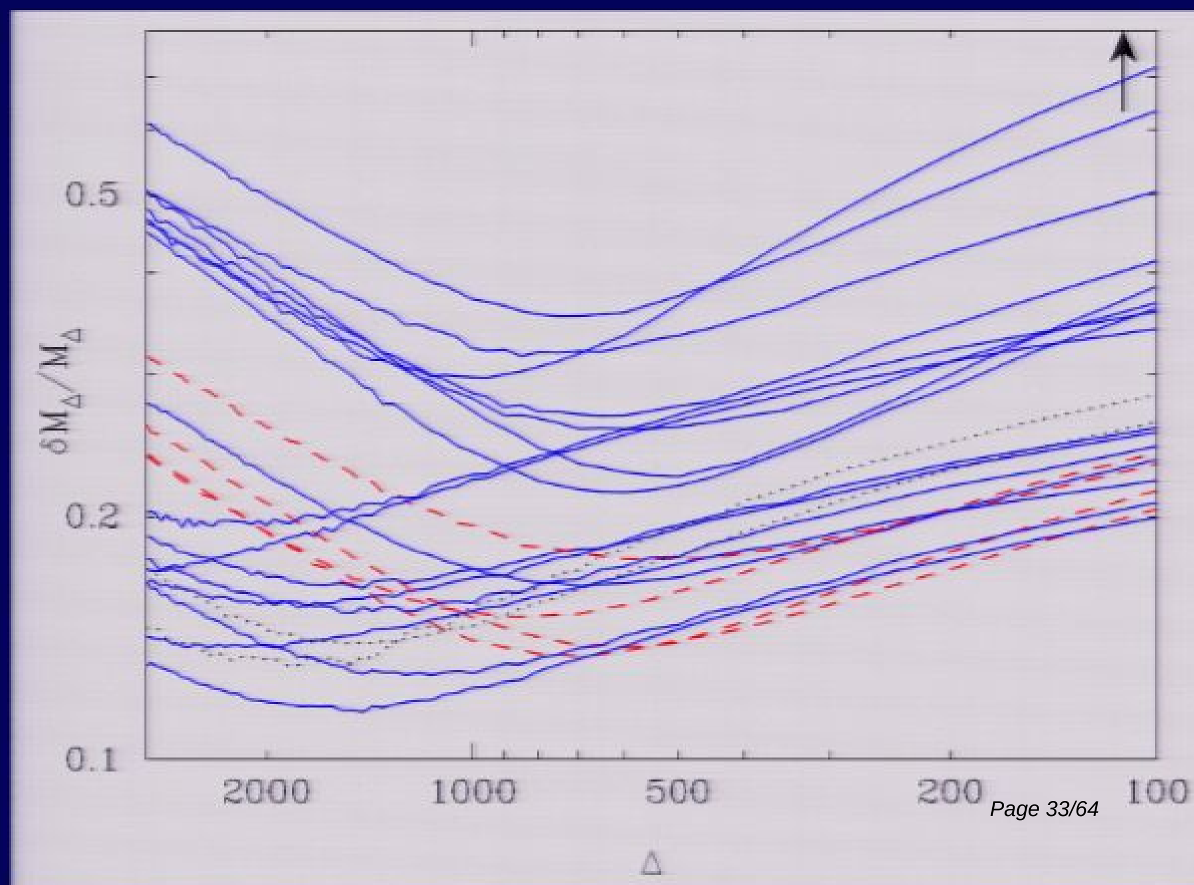

First SZA+LoCuSS Results: M_{WL} – Y

SZA detections of 25/30 clusters

- 3 contaminated by radio emission, 2 peculiar objects in Subaru sample
- 18 of 25 have NFW fits
- First results: $Y(r_{\Delta,WL})$ vs. M_{WL}
- Sample can be enlarged:
  - Disturbed clusters (Okabe & Umetsu 2008)
  - Aperture masses from integrated shear (non-parametric)
- Self-similar prediction for Mass-Y scaling relation:

$$Y_\Delta D_A^2 E(z)^{-2/3} \propto \Delta^{1/3} f_{gas,\Delta} M_\Delta^{5/3}$$

First SZA+LoCuSS Results: M_{WL} – Y

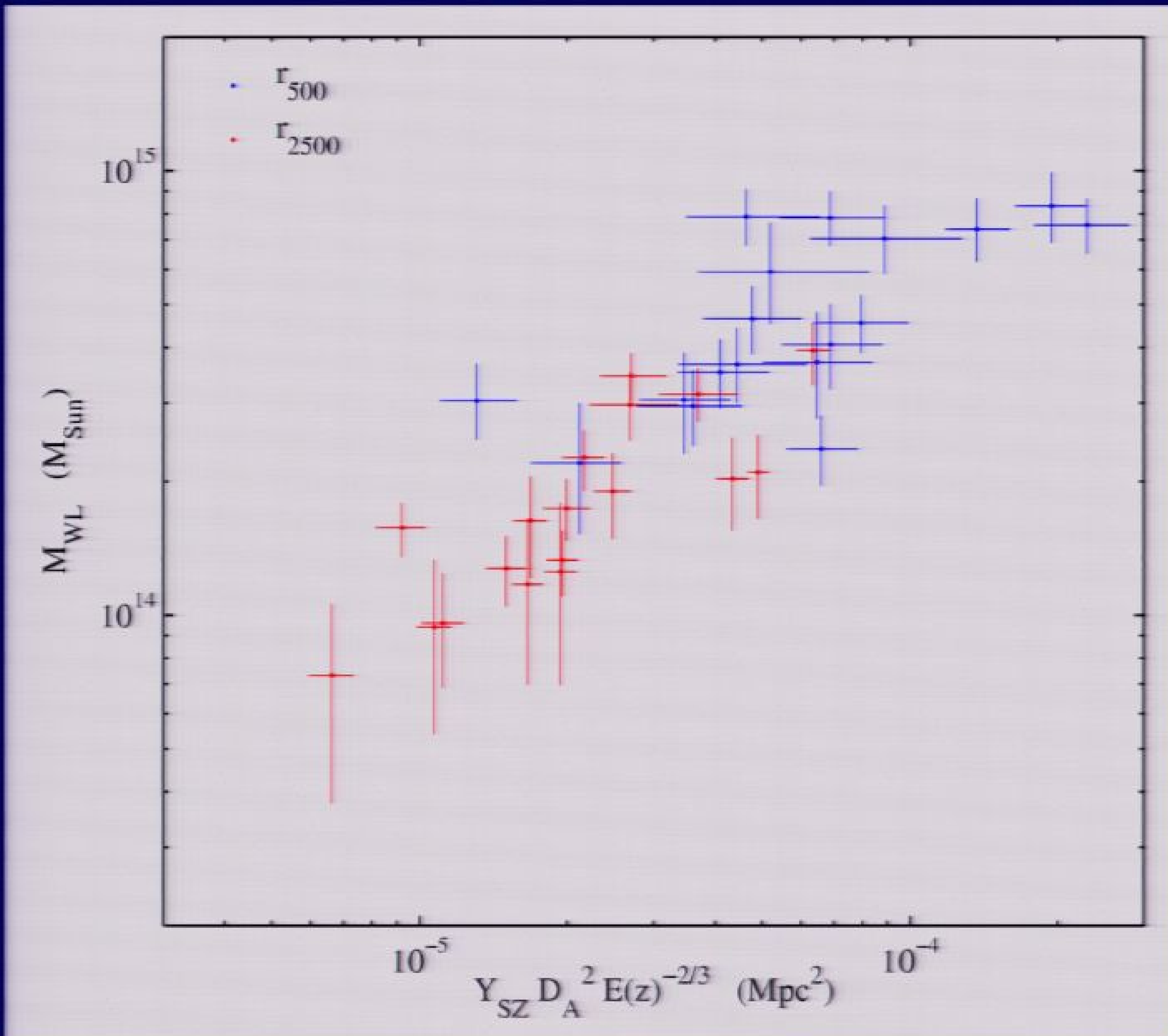

First SZA+LoCuSS Results: M_{WL} – Y

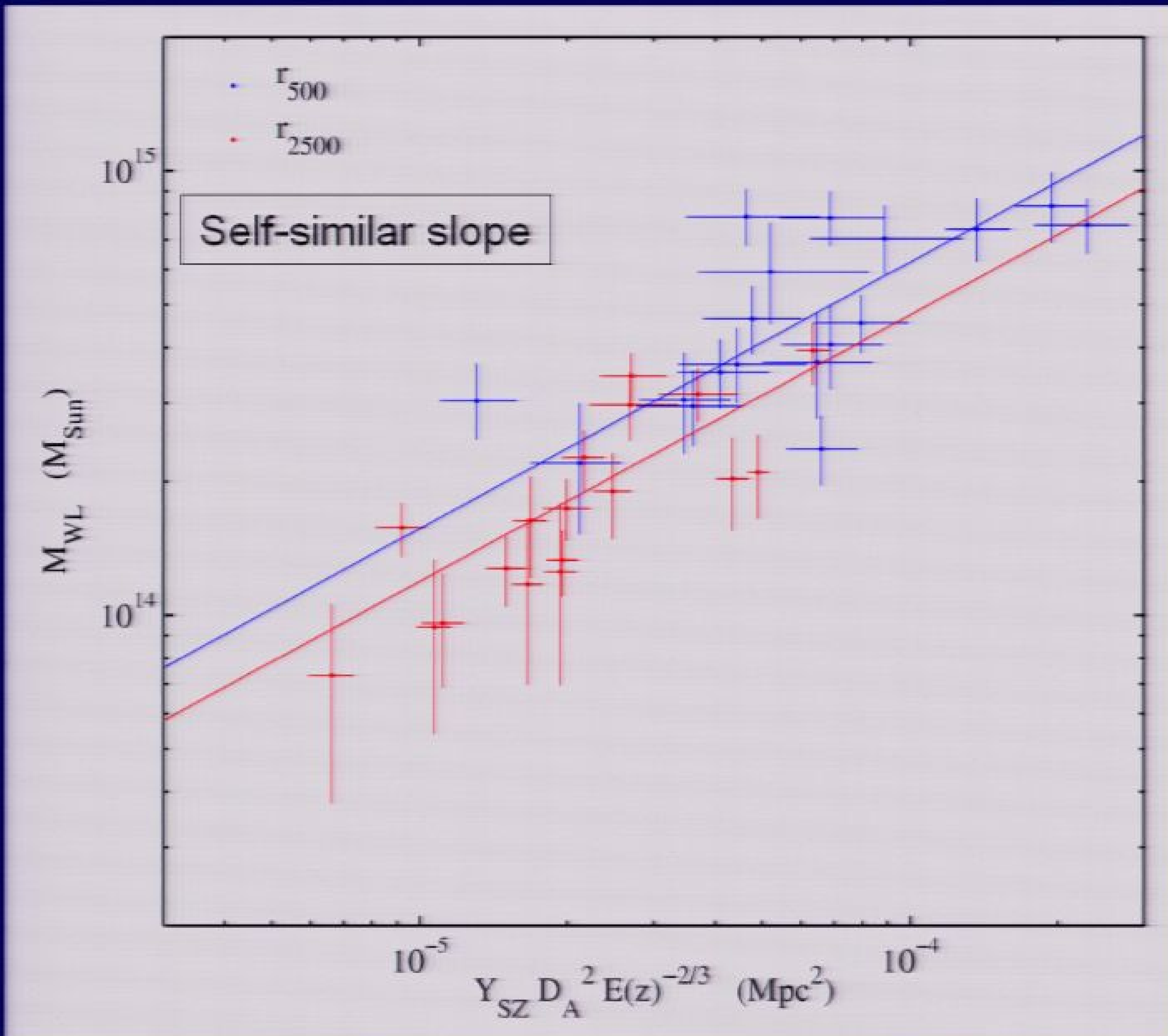

First SZA+LoCuSS Results: M_{WL} – Y

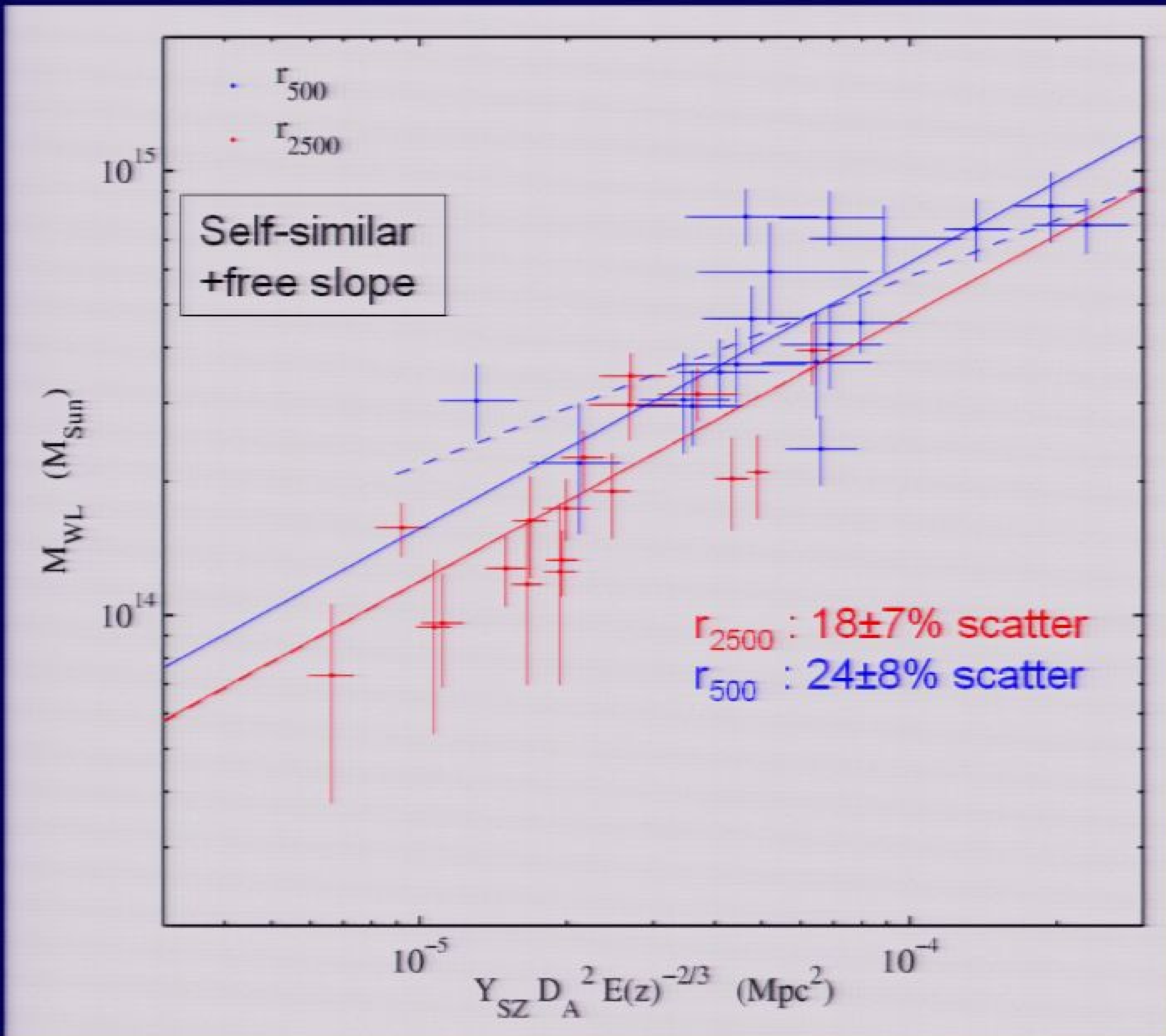

First SZA+LoCuSS Results: M_{WL} – Y

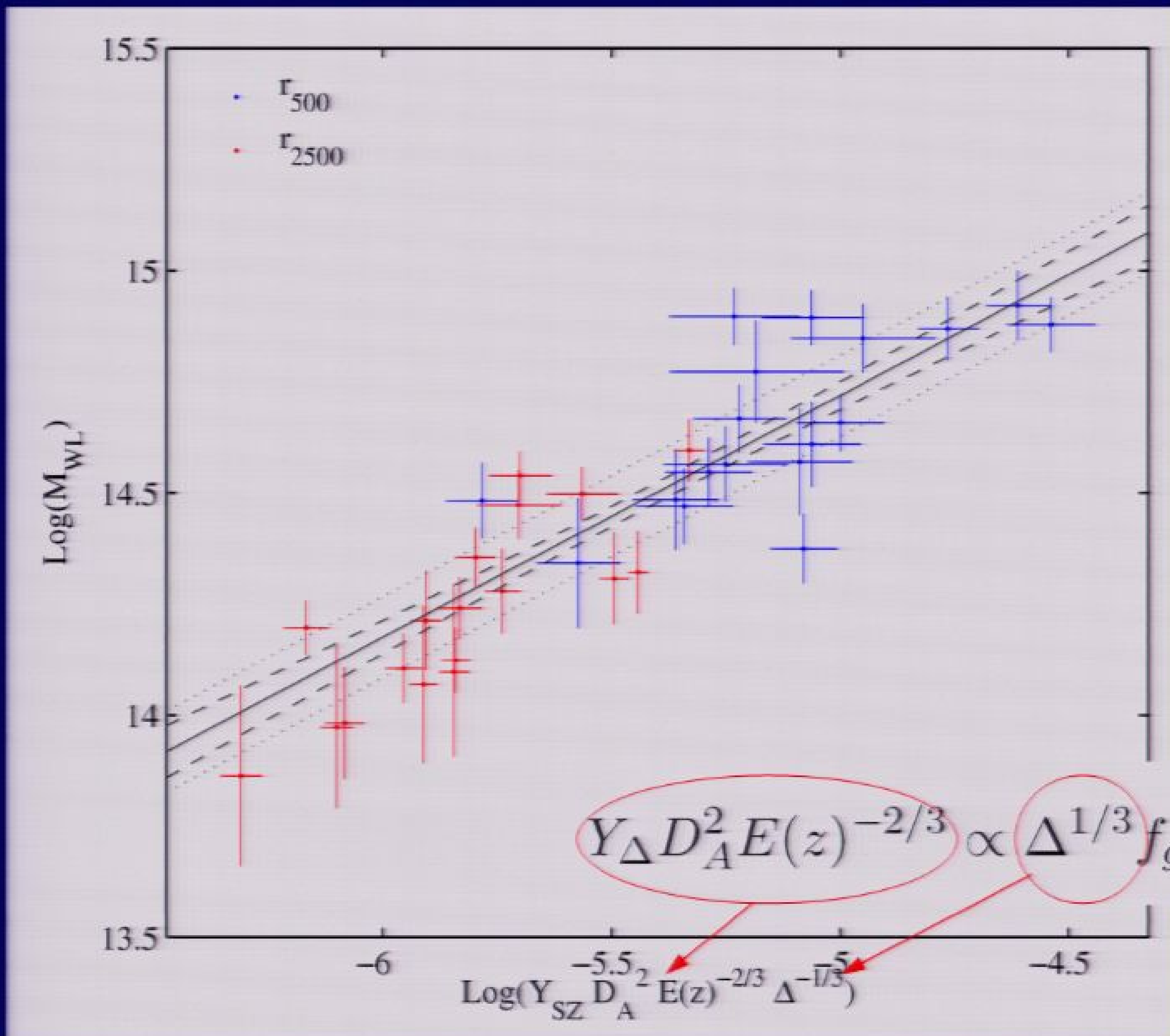

$$Y_\Delta D_A^2 E(z)^{-2/3} \propto \Delta^{1/3} f_{gas,\Delta} M_\Delta^{5/3}$$

First SZA+LoCuSS Results: M_{WL} – Y

First M_{WL} – Y scaling relation:

- Consistent with self similarity at r_{2500} and r_{500}
- Scatter larger (~20%) than theoretical (8%)
- Must account for:
  - Model-induced scatter
  - Scatter from mass (or SZ) projection

Improvements in mass precision from WL+SL combination

First SZA+LoCuSS Results: M_{WL} – Y

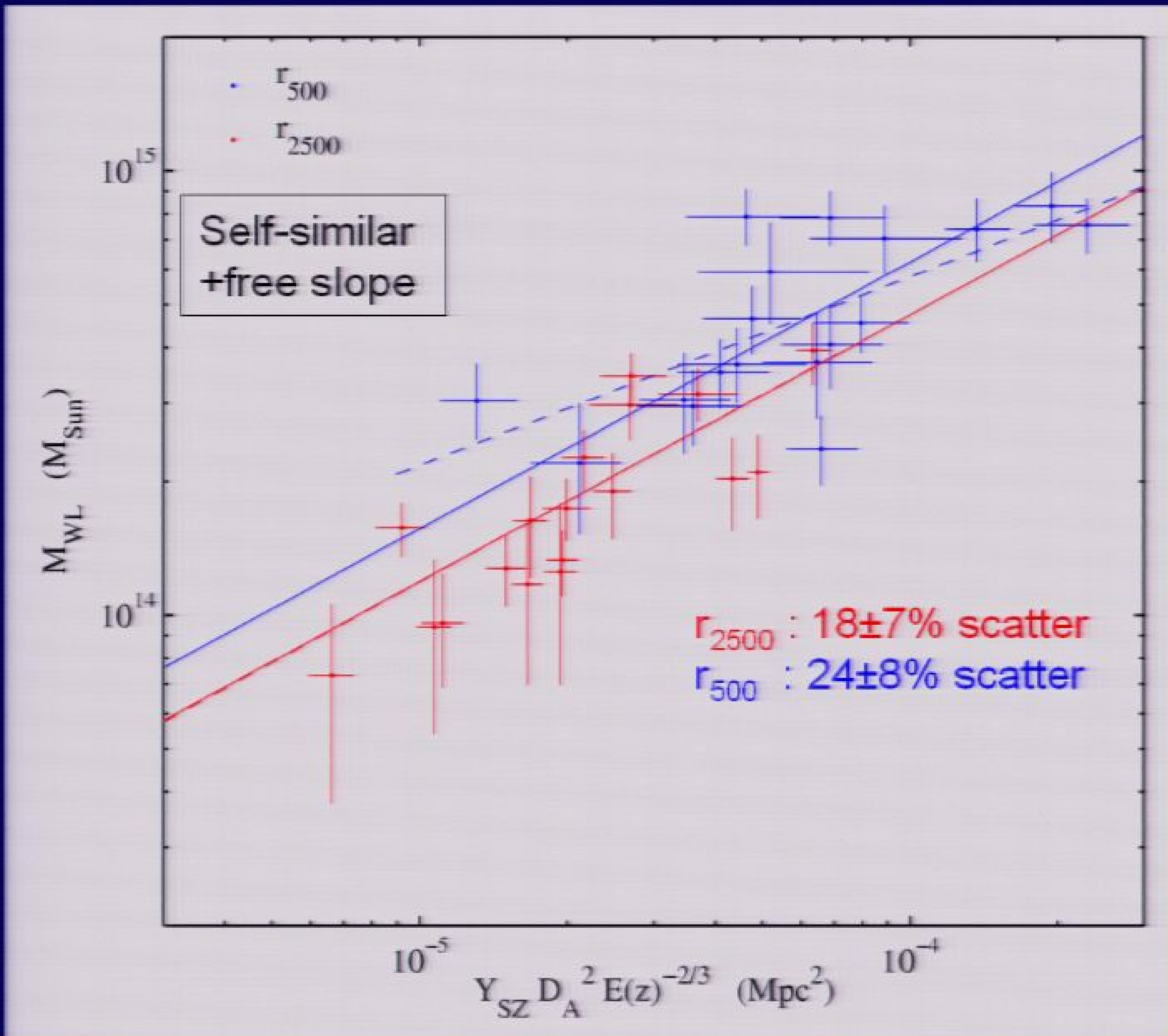

First SZA+LoCuSS Results: M_{WL} – Y

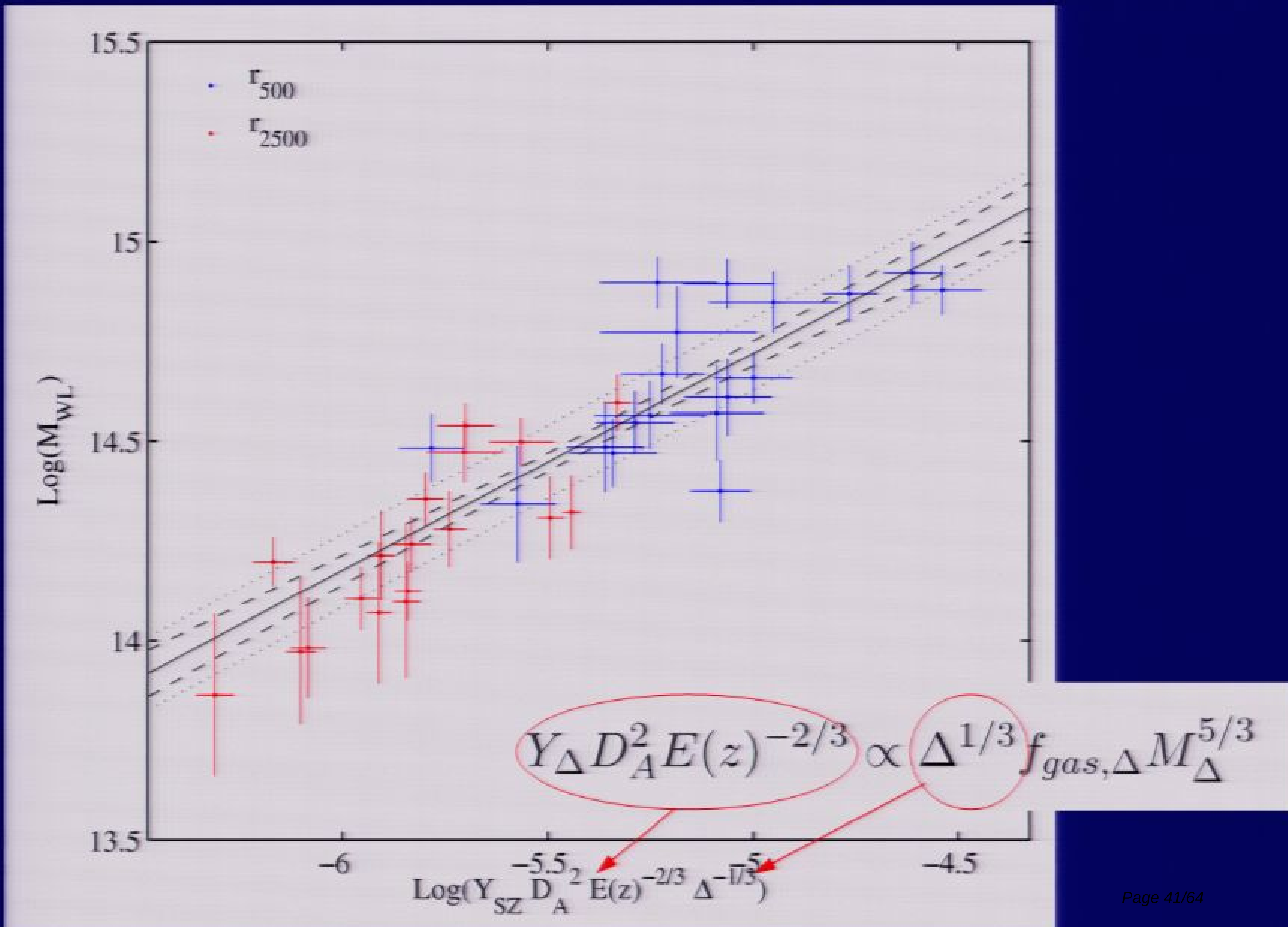

First SZA+LoCuSS Results: M_{WL} – Y

First M_{WL} – Y scaling relation:

- Consistent with self similarity at r_{2500} and r_{500}
- Scatter larger (~20%) than theoretical (8%)
- Must account for:
  - Model-induced scatter
  - Scatter from mass (or SZ) projection

Improvements in mass precision from WL+SL combination

First SZA+LoCuSS Results: M_{WL} – Y

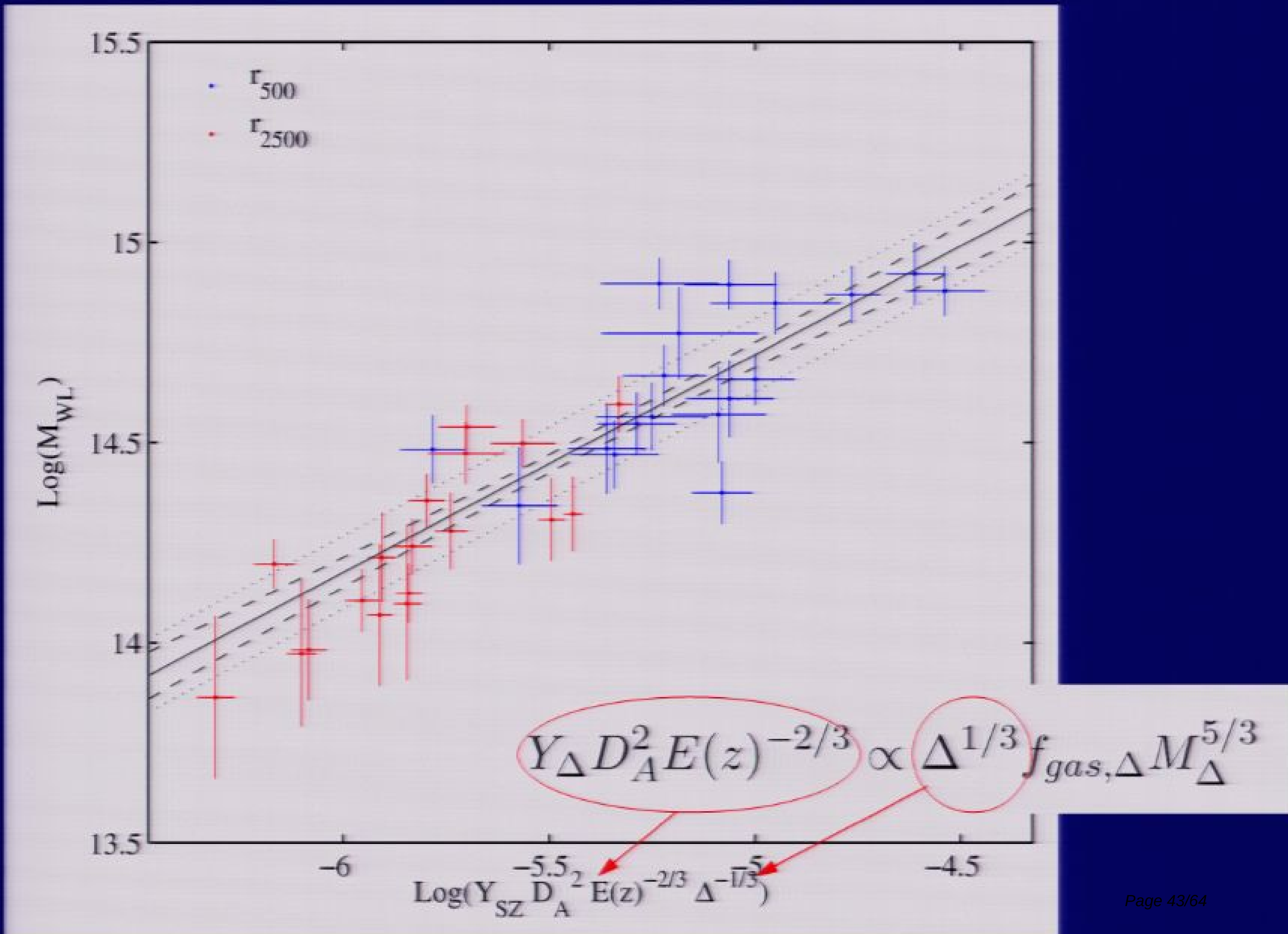

PI SZ Universe
April 28, 2009

First SZA+LoCuSS Results: M_{WL} – Y

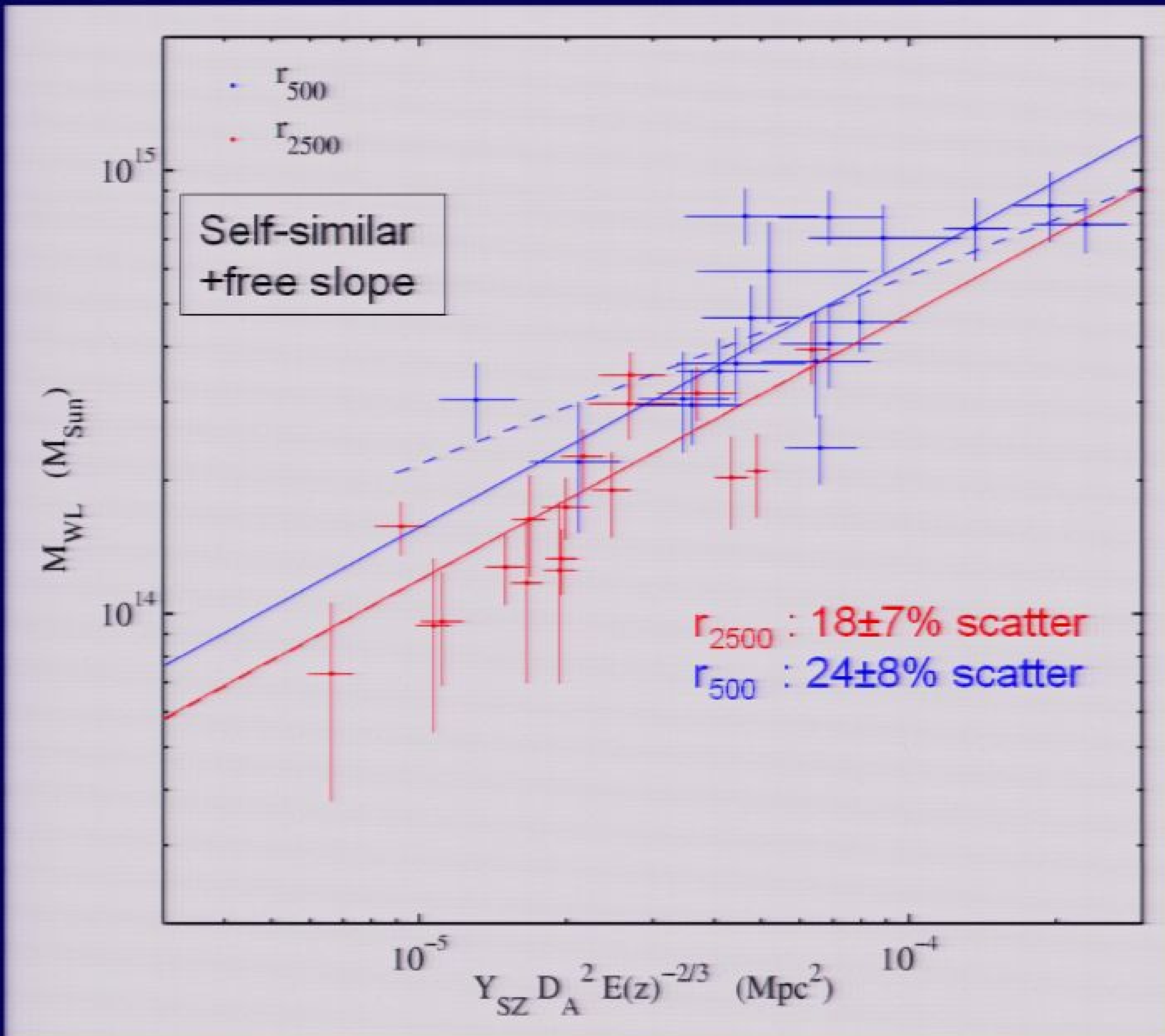

First SZA+LoCuSS Results: $M_{WL} - Y$

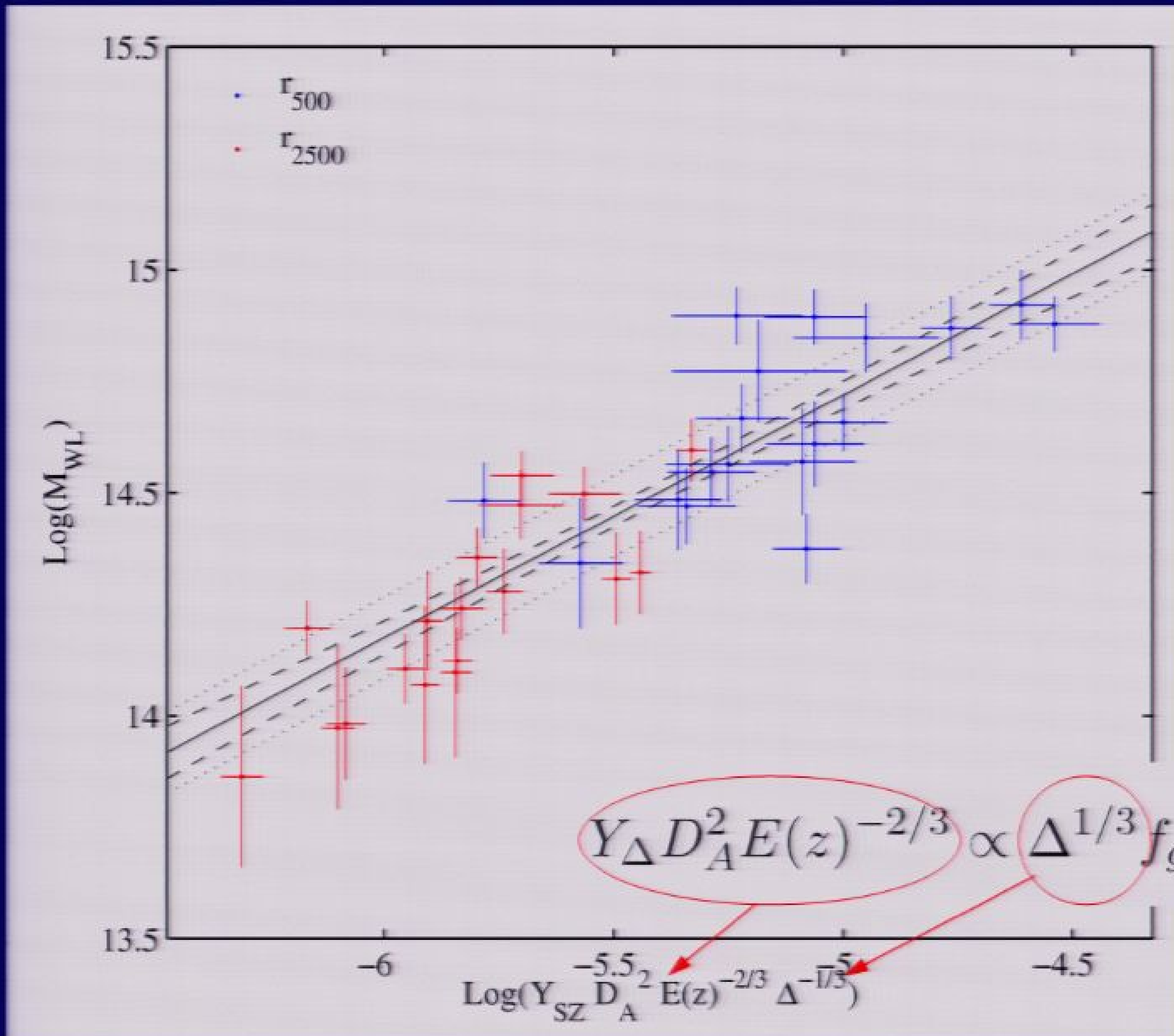

$$Y_\Delta D_A^2 E(z)^{-2/3} \propto \Delta^{1/3} f_{gas,\Delta} M_\Delta^{5/3}$$

CMB Temperature Anisotropy at $\ell \sim 4000$

Matthew Sharp, PhD (2008)

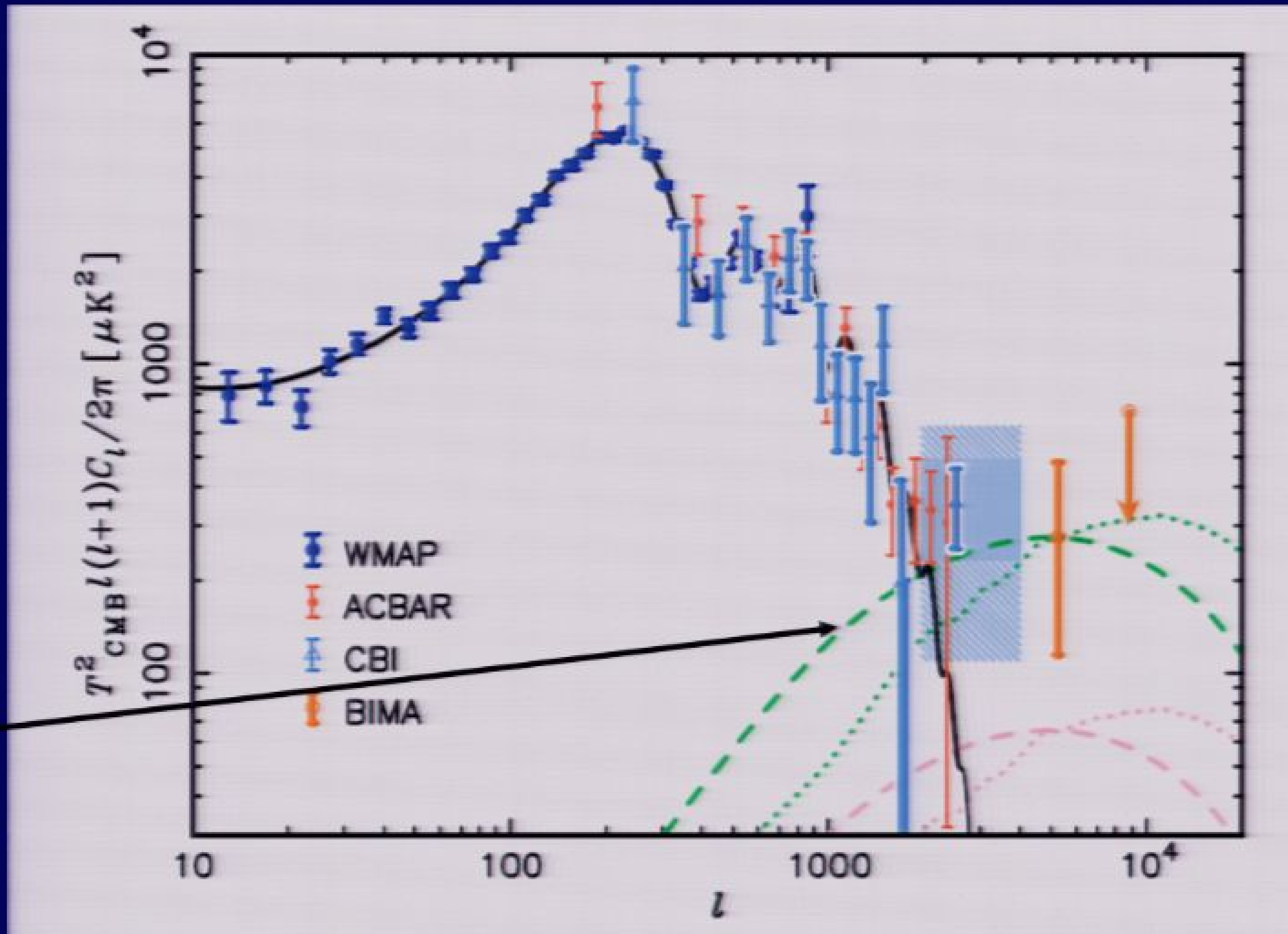

Secondary anisotropy from SZE

$C_l \sim \sigma_8^{\,7}$ (Komatsu&Seljak 2002)

First SZA+LoCuSS Results: M_{WL} – Y

First M_{WL} – Y scaling relation:

- Consistent with self similarity at r_{2500} and r_{500}
- Scatter larger (~20%) than theoretical (8%)
- Must account for:
  - Model-induced scatter
  - Scatter from mass (or SZ) projection

Improvements in mass precision from WL+SL combination

CMB Temperature Anisotropy at ℓ~4000

Matthew Sharp, PhD (2008)

Secondary anisotropy from SZE

$C_l \sim \sigma_8^7$ (Komatsu&Seljak 2002)

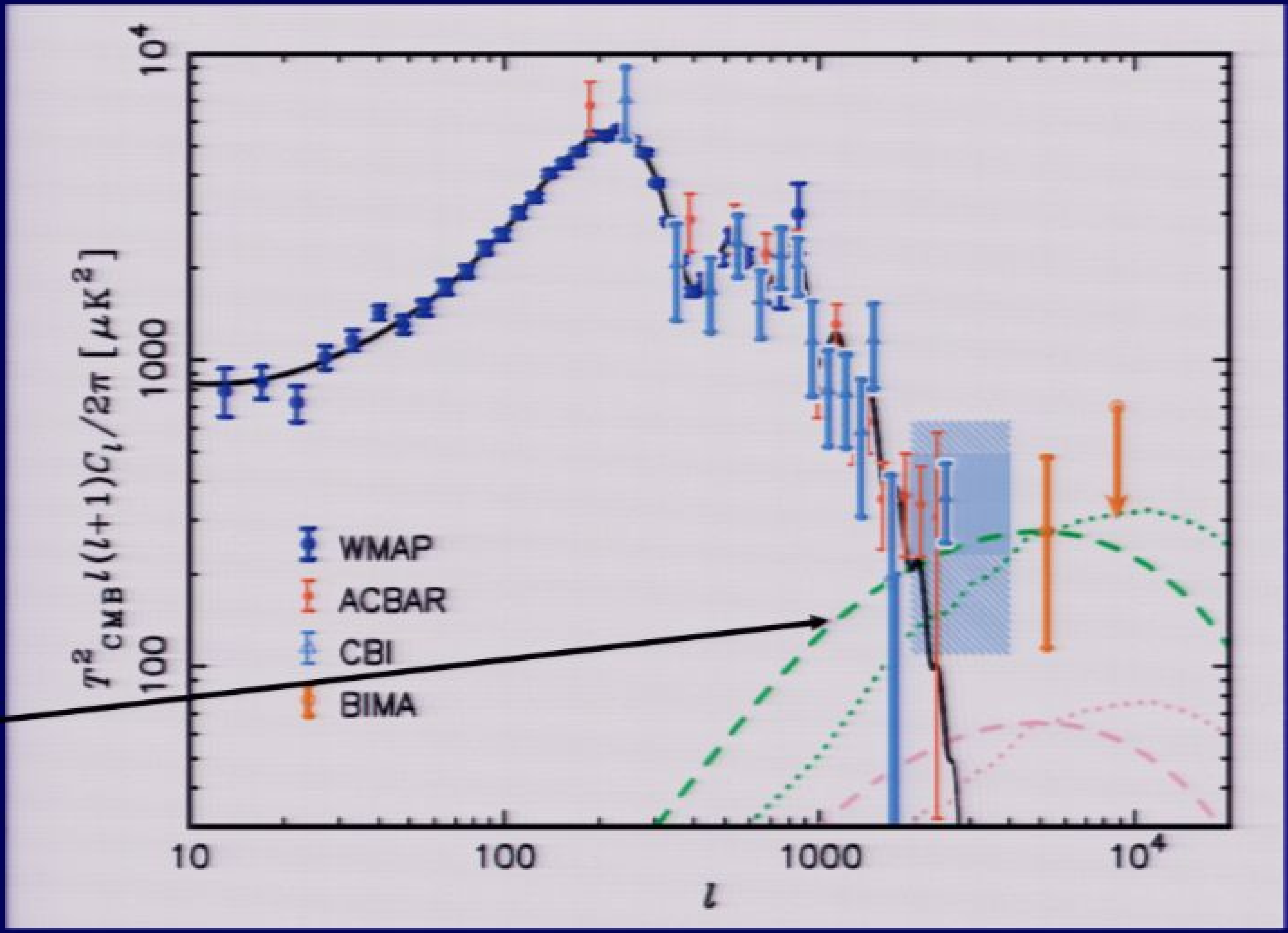

CMB Temperature Anisotropy at ℓ~4000

Matthew Sharp, PhD (2008)

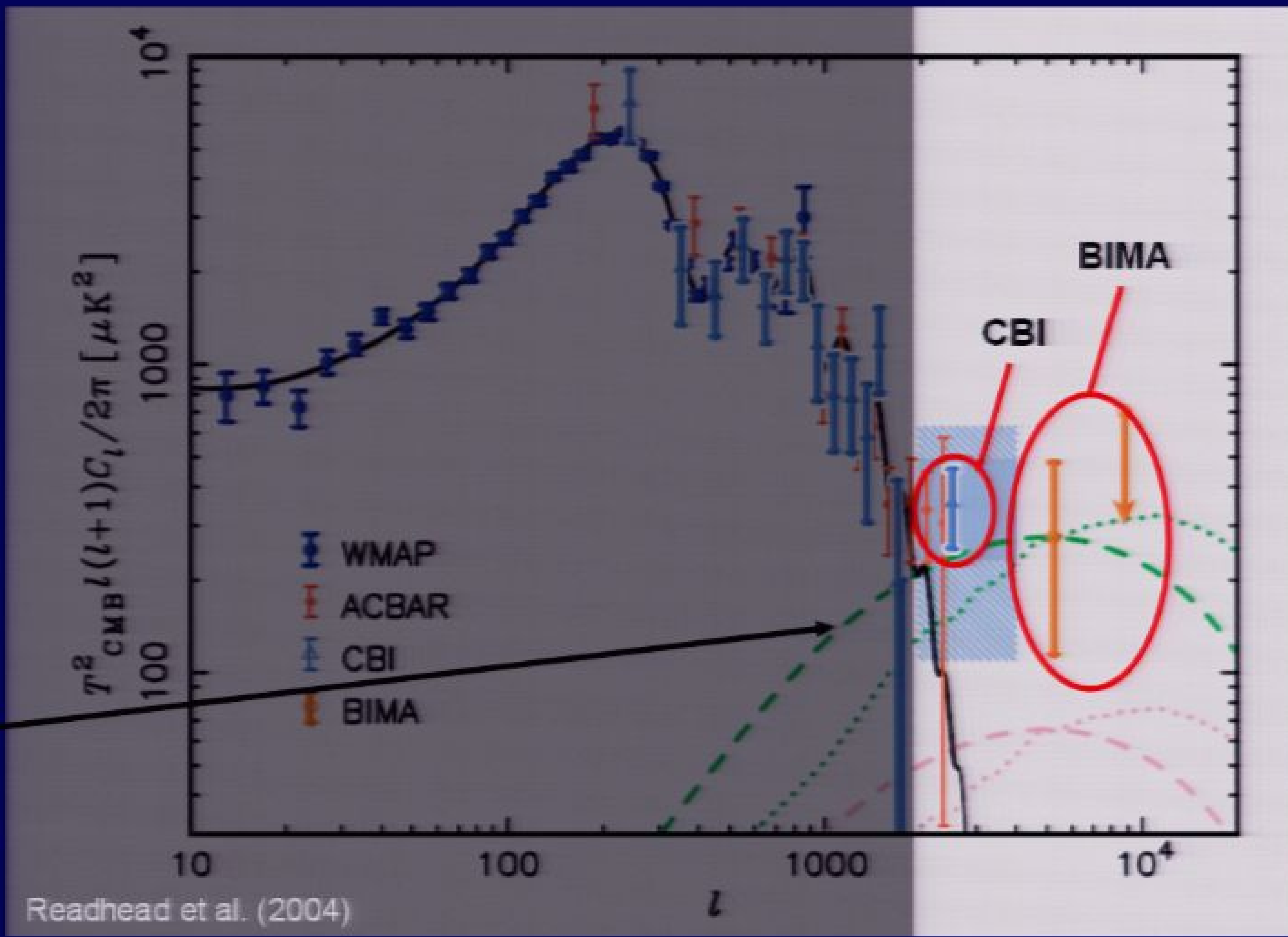

Secondary anisotropy from SZE

$C_l \sim \sigma_8^{\,7}$ (Komatsu&Seljak 2002)

CMB Temperature Anisotropy at ℓ~4000

Matthew Sharp, PhD (2008)

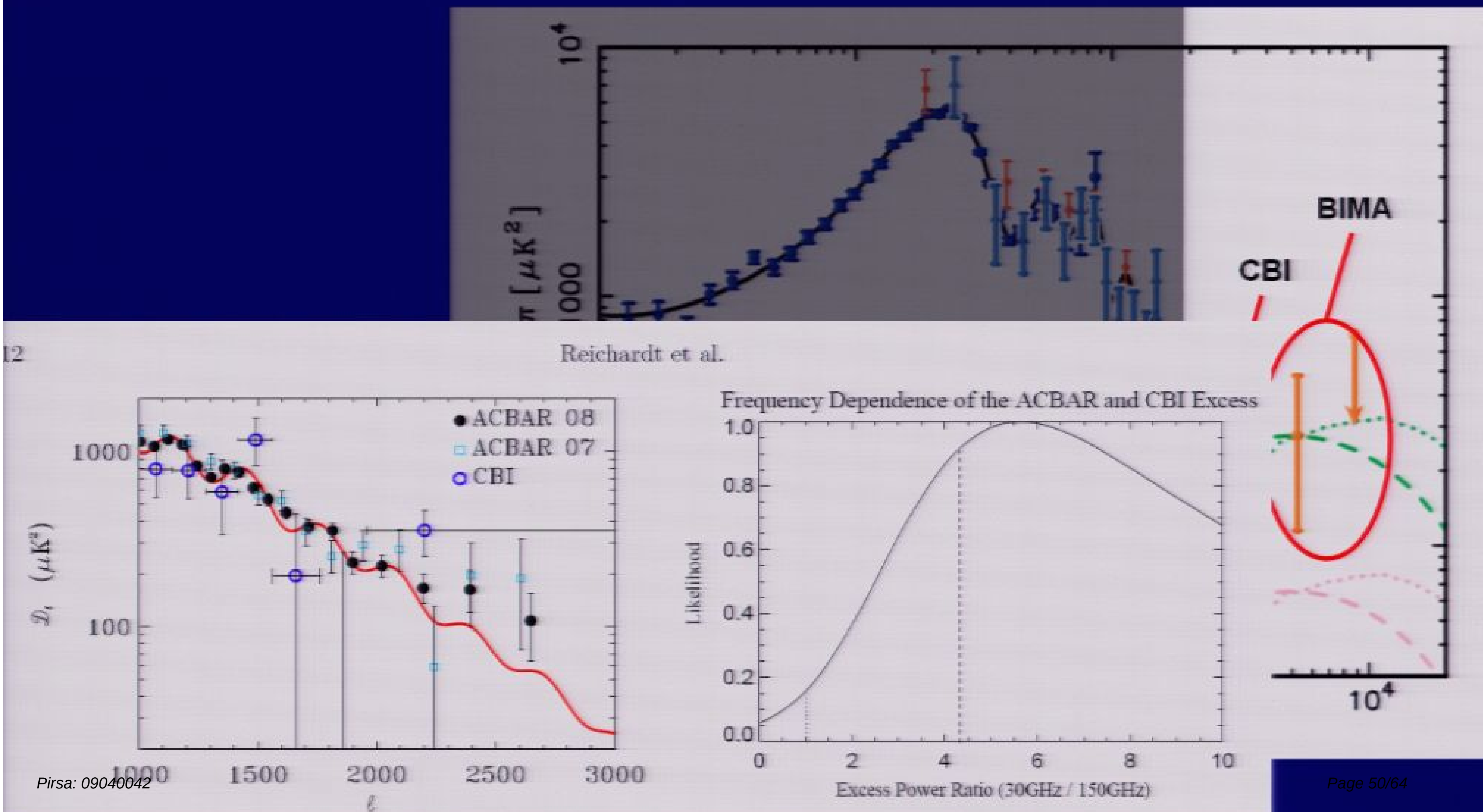

CMB Temperature Anisotropy at ℓ~4000

Matthew Sharp, PhD (2008)

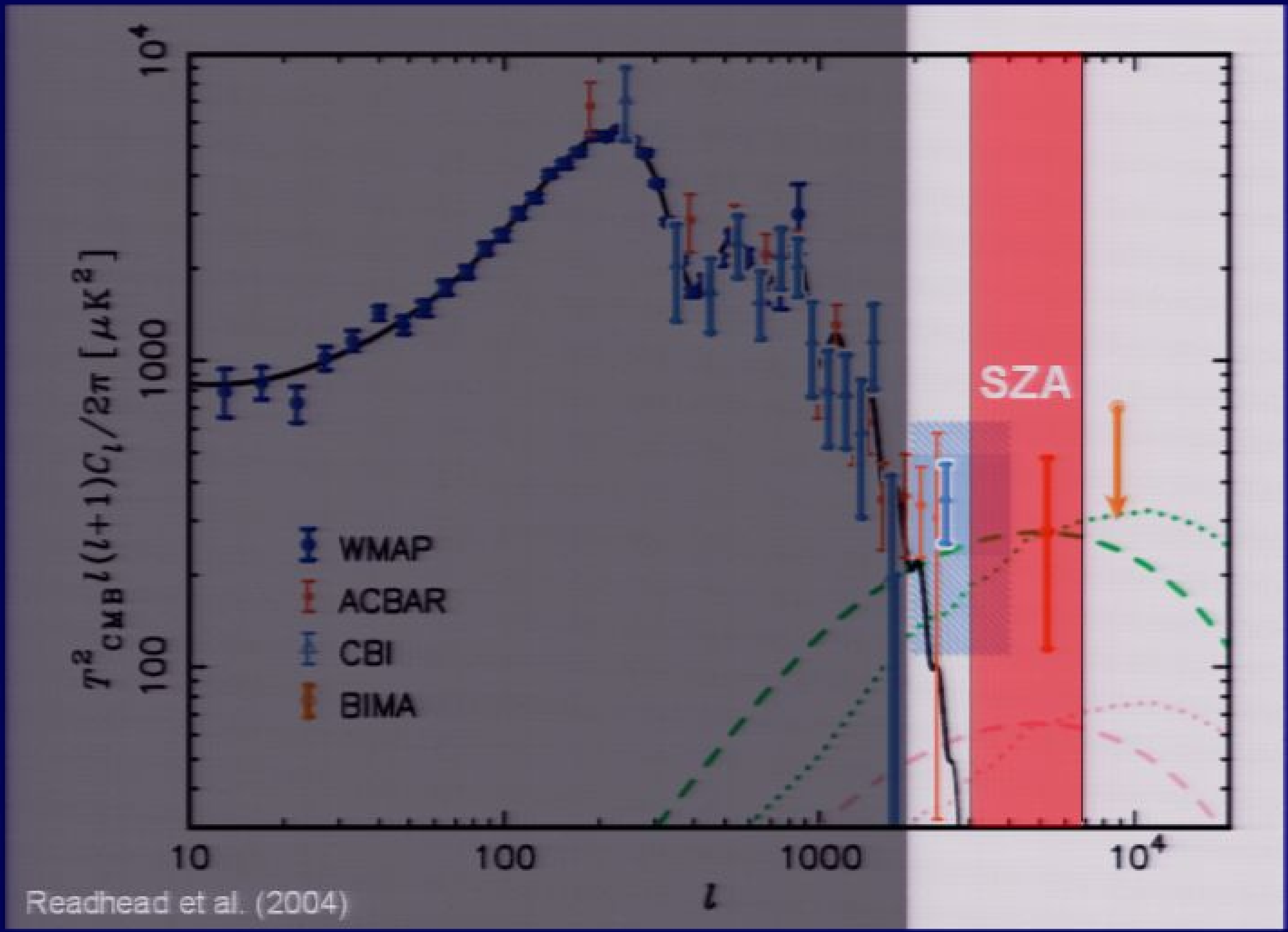

SZA Anisotropy Observations

12 Groups of 4 fields

- Selected without extragalactic priors
- Lead-trail-trail-trail arrangement for ground subtraction

1.5 square degrees

1340 Hours of SZA time

- Typical map rms:
  - 0.2 mJy (short baselines)
  - 0.15 mJy (all baselines)

Window function →

- Mean l = 4066
- 68%: 2930-5880

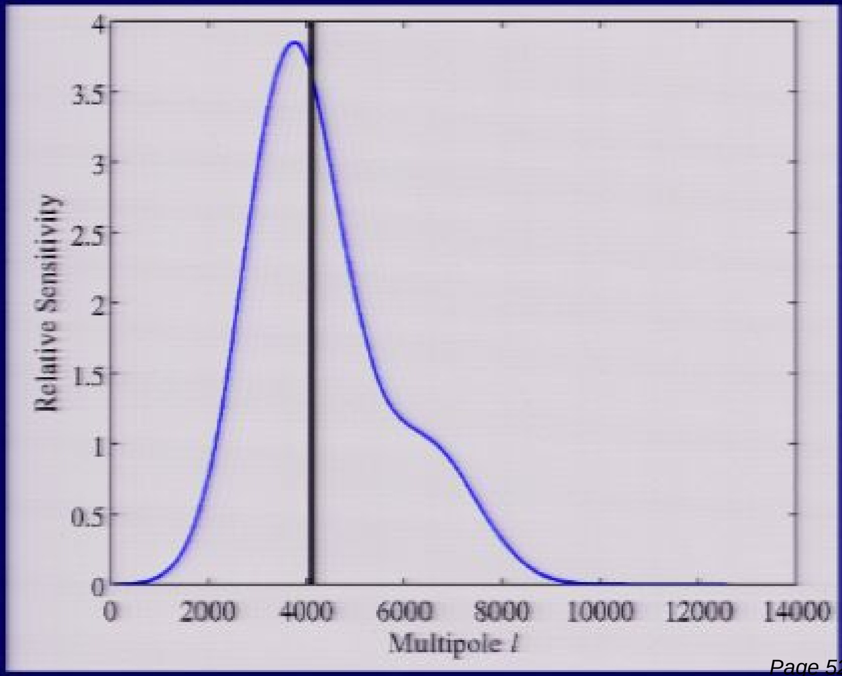

Radio Source Contamination

Point source contribution increases like l^2 – must remove carefully

Mode removal technique (Bond et al. 1998, Halverson et al. 2002)

- Requires position only
- Three components used per source to account for unknown spectrum

Combination of techniques

- SZA long+short baselines – 30 GHz detection to ~600μJy
- Deep (30μJy) 8 GHz survey with VLA
  - Account for sources below 30 GHz detection limit
- (1.4 GHz from NVSS/FIRST for 2 fields without 8 GHz)

Residual power estimated from simulation

- Radio source populations from SZA cluster survey, deZotti et al. (2005)
- Expected to be insignificant (20 μK^2 calculated)

Jackknife Tests

Three ways to split the data into "identical" halves

- Frequency (alternating bands)
- Time (first and second half of observing period)
- Time (alternating days)

Ground subtraction required to pass frequency JK

Jackknife Test	Power [μK^2]	PTE
Frequency	65^{+70}_{-40}	0.19
First–Second Half	-25^{+106}_{-81}	0.59
Even–Odd Days	-40^{+96}_{-49}	0.41

Jackknife Tests

Three ways to split the data into "identical" halves

- Frequency (alternating bands)
- Time (first and second half of observing period)
- Time (alternating days)

Ground subtraction required to pass frequency JK

Jackknife Test	Power [μK^2]	PTE
Frequency	65^{+70}_{-40}	0.19
First–Second Half	-25^{+106}_{-81}	0.59
Even–Odd Days	-40^{+96}_{-49}	0.41
Unjackknifed Data	60^{+65}_{-55}	0.12

SZA Anisotropy Measurement

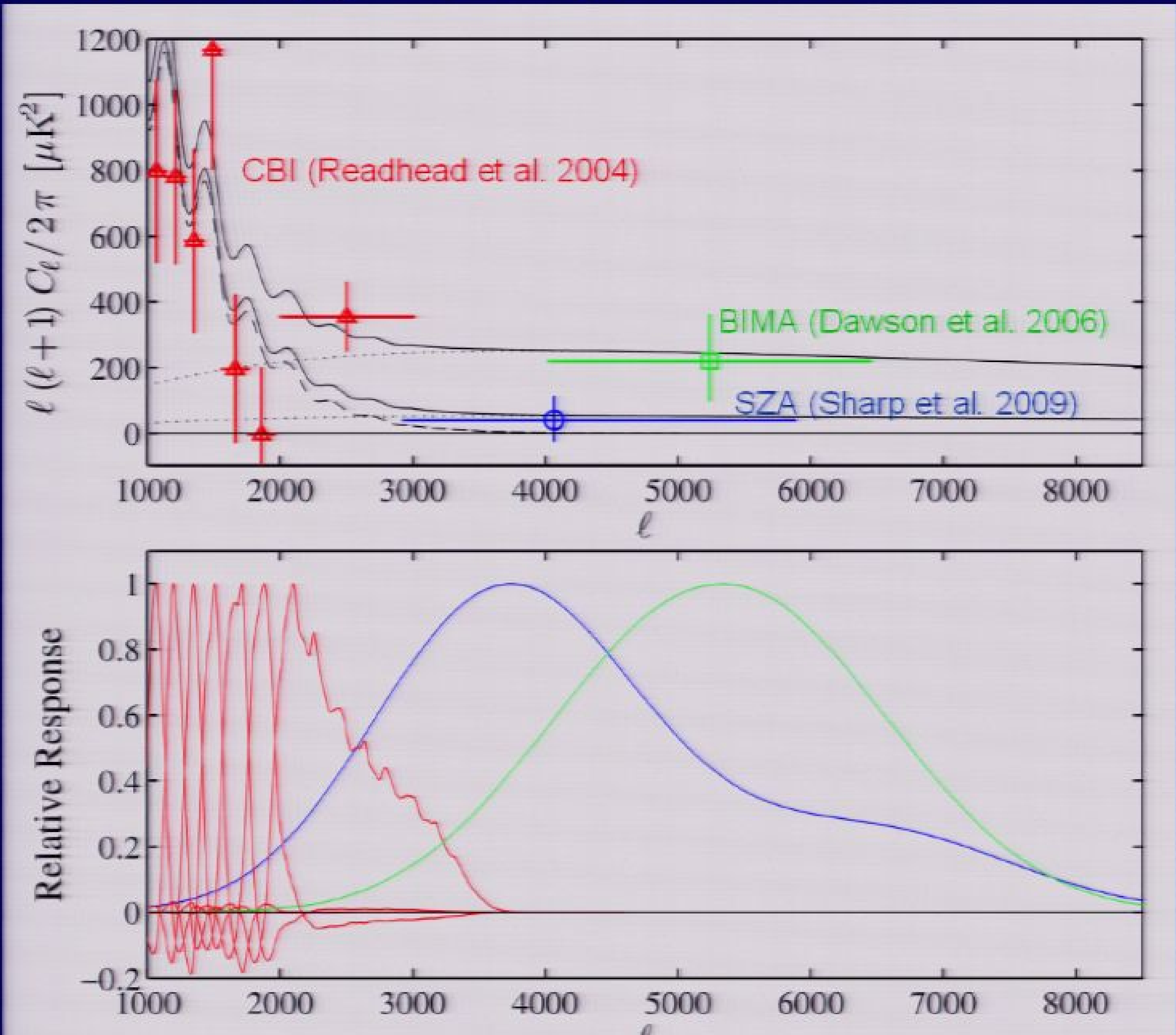

Anisotropy Contributions

Start with:

Unjackknifed Data	60^{+65}_{-55}

Account for other sources of power:

Source	Power Contribution [μK^2]
Primary CMB	26 ± 5
Undetected Radio Sources	20 ± 28
Galactic Synchrotron and Free-Free	2
Galactic Spinning Dust	< 16

Leftovers due to SZE:

Secondary CMB (SZE)	14^{+71}_{-62}
and upper limit at 95% C.L.	149

For σ_8=0.8, cosmic variance contributes additional 50% to error

SZA Anisotropy Measurement

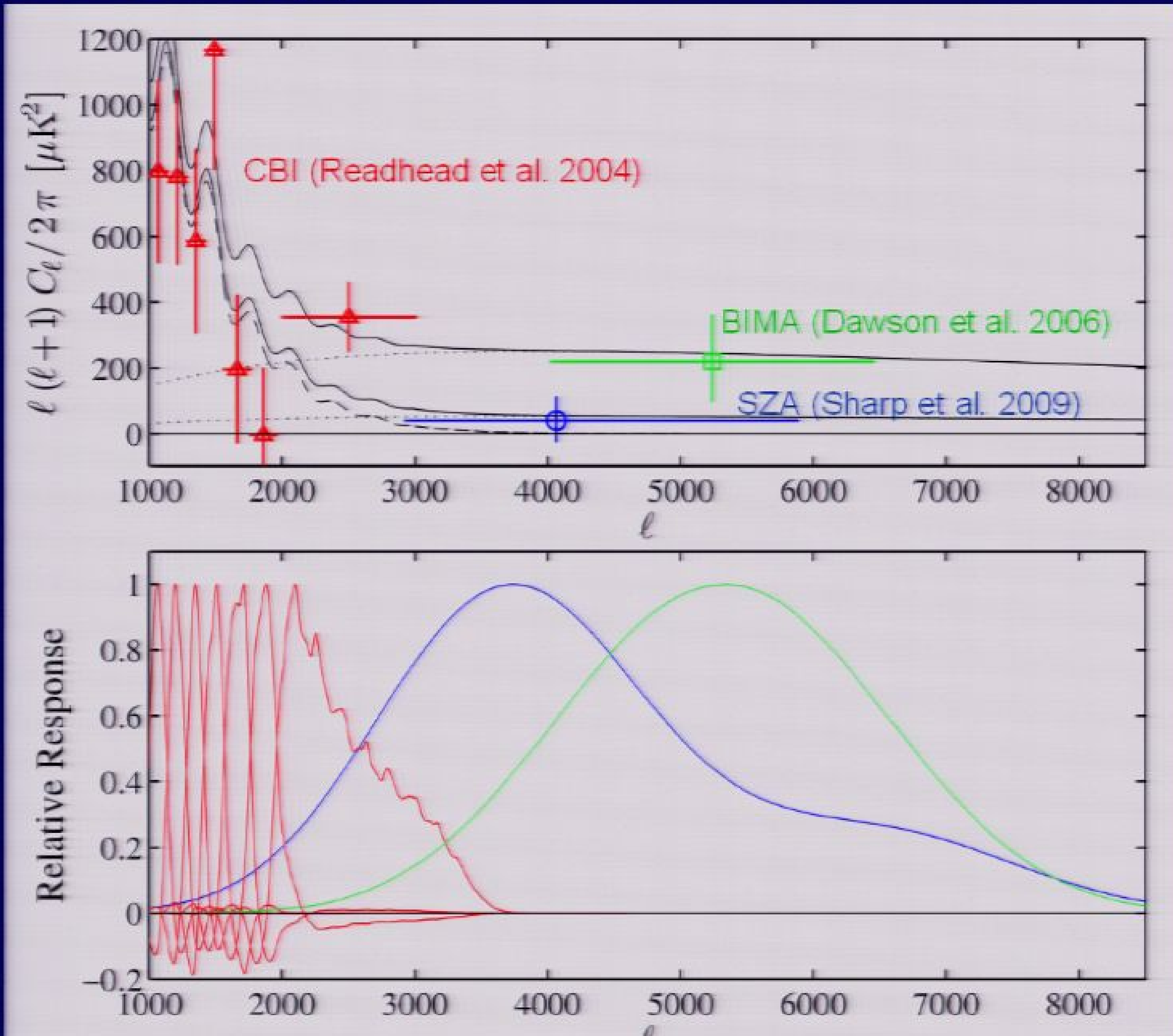

Anisotropy Contributions

Start with:

Unjackknifed Data	60^{+65}_{-55}

Account for other sources of power:

Source	Power Contribution [μK^2]
Primary CMB	26 ± 5
Undetected Radio Sources	20 ± 28
Galactic Synchrotron and Free-Free	2
Galactic Spinning Dust	< 16

Leftovers due to SZE:

Secondary CMB (SZE)	14^{+71}_{-62}
and upper limit at 95% C.L.	149

For σ_8=0.8, cosmic variance contributes additional 50% to error

What about σ_8?

- As we saw yesterday, this is *highly* dependent on simulation/model

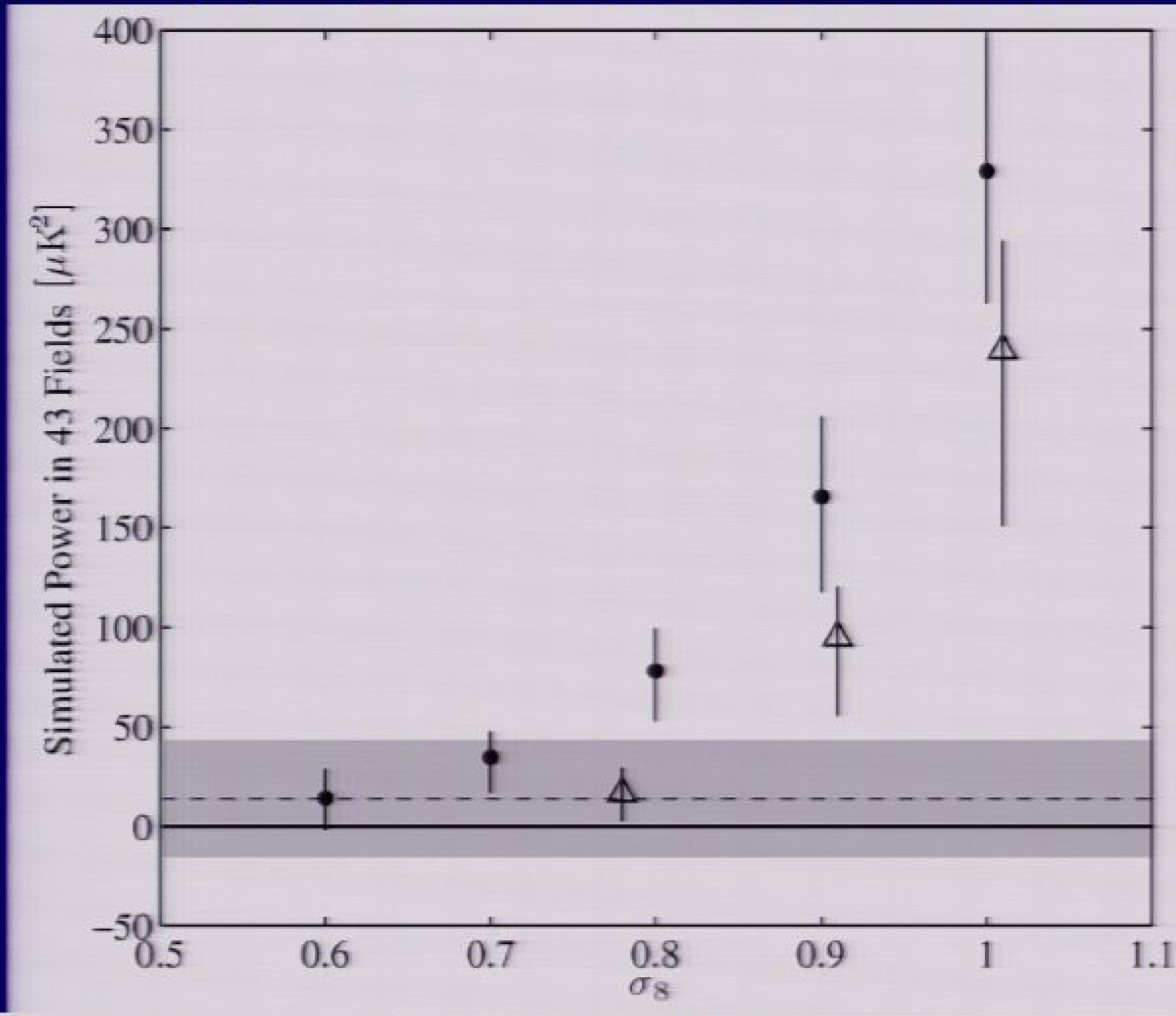

Holder et al. (2007) are shown for multiple values of σ_8 as solid dots, while triangles indicate the simulations of Shaw et al. (2007), White et al. (2002) and Schulz & White (2003) with $\sigma_8 =$ 0.77, 0.9, and 1.0, respectively.

Anisotropy Contributions

Start with:

Unjackknifed Data	60^{+65}_{-55}

Account for other sources of power:

Source	Power Contribution $[\mu K^2]$
Primary CMB	26 ± 5
Undetected Radio Sources	20 ± 28
Galactic Synchrotron and Free-Free	2
Galactic Spinning Dust	< 16

Leftovers due to SZE:

Secondary CMB (SZE)	14^{+71}_{-62}
and upper limit at 95% C.L.	149

For σ_8=0.8, cosmic variance contributes additional 50% to error

What about σ_8?

- As we saw yesterday, this is *highly* dependent on simulation/model

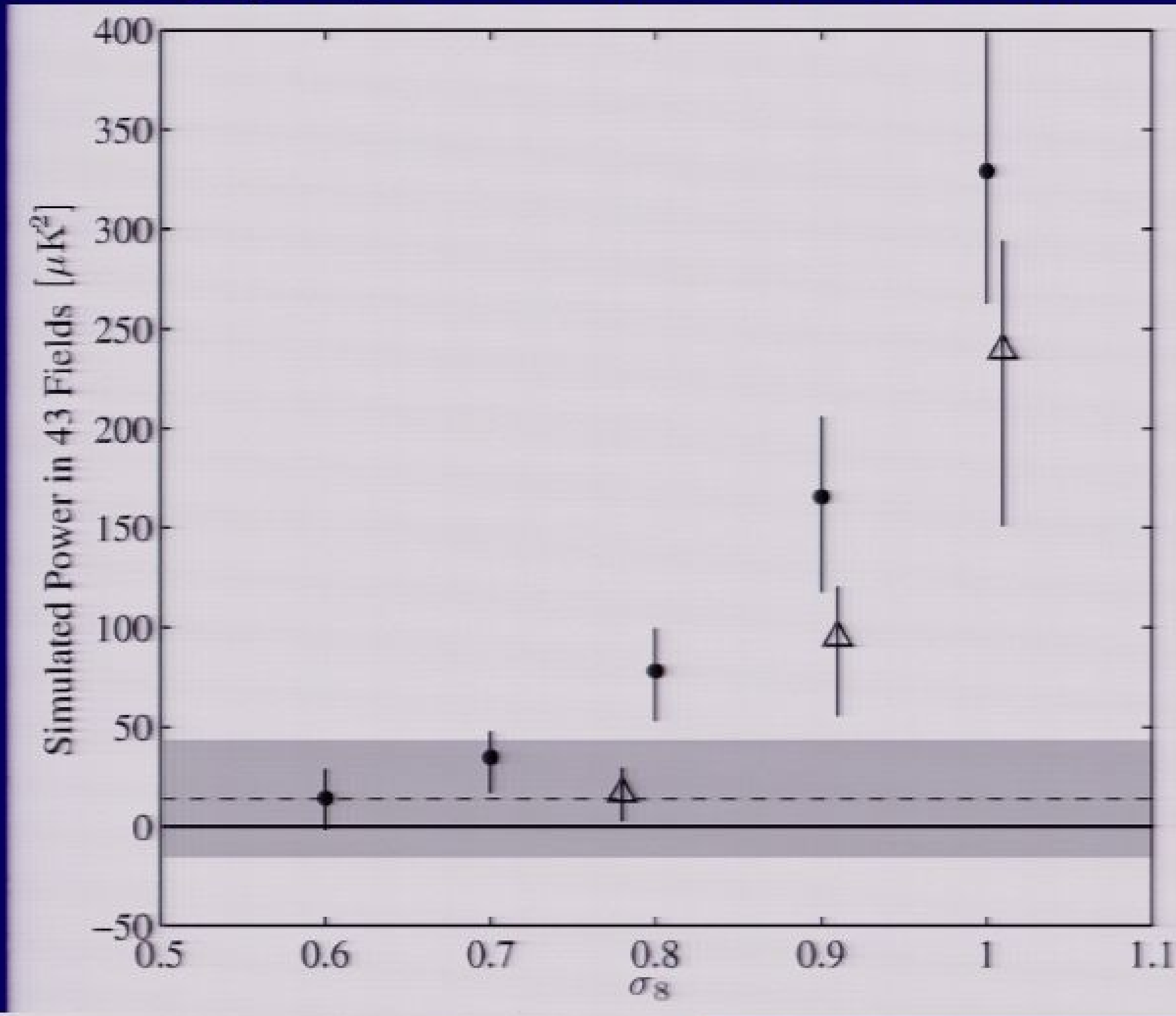

Holder et al. (2007) are shown for multiple values of σ_8 as solid dots, while triangles indicate the simulations of Shaw et al. (2007), White et al. (2002) and Schulz & White (2003) with σ_8 = 0.77, 0.9, and 1.0, respectively.

What about σ_8?

- As we saw yesterday, this is *highly* dependent on simulation/model

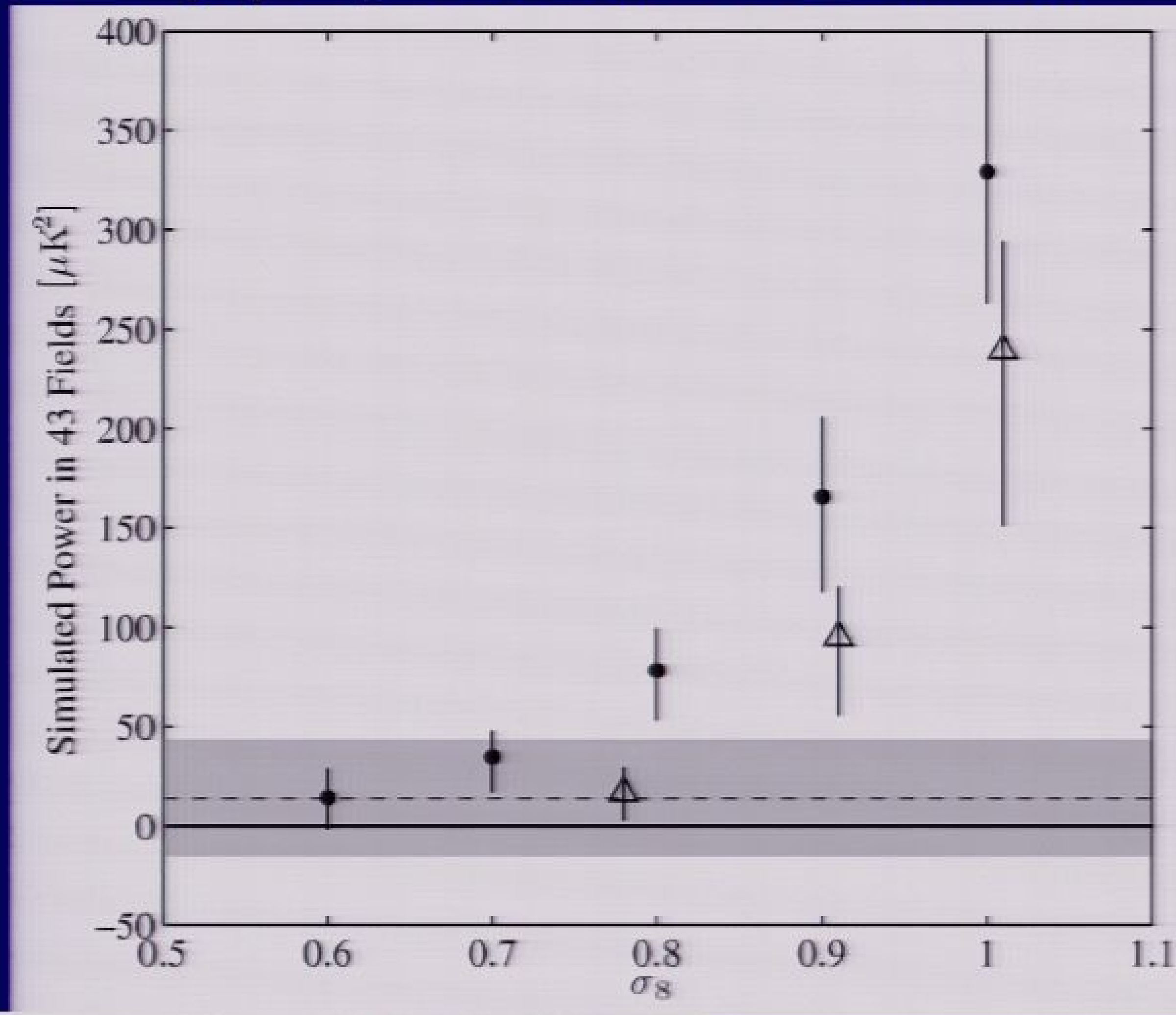

Holder et al. (2007) are shown for multiple values of σ_8 as solid dots, while triangles indicate the simulations of Shaw et al. (2007), White et al. (2002) and Schulz & White (2003) with σ_8 = 0.77, 0.9, and 1.0, respectively.